Fuzzy Gain Scheduled Fractional-Order PID Temperature Control of a Continuous Stirred Tank Reactor Process

Rahel Fitwi Gebrekirstos

A Thesis Submitted to

The Department of Electrical Power and Control Engineering

School of Electrical Engineering and Computing

Presented in Partial Fulfillment of the Requirement for the Degree of Master of Science in Electrical Power and Control engineering (Control Engineering)

Office of Graduate Studies

Adama Science and Technology University

September, 2021

Adama, Ethiopia

Fuzzy Gain Scheduled Fractional-Order PID Temperature Control of a Continuous Stirred Tank Reactor Process

Rahel Fitwi Gebrekirstos

Advisor: Prof. Gang Gyoo Jin
Co-advisor: Mr. Minyamer Gelawe Wase (MSc.)

A Thesis Submitted to
The Department of Electrical Power and Control Engineering
School of Electrical Engineering and Computing

Presented in Partial Fulfillment of the Requirement for the Degree of Master of Science in Electrical Power and Control engineering (Control Engineering)

Office of Graduate Studies
Adama Science and Technology University

September, 2021
Adama, Ethiopia

DECLARATION

I hereby declare that this Master Thesis entitled "Fuzzy Gain Scheduled Fractional-Order PID Temperature Control of a Continuous Stirred Tank Reactor Process" is my original work. That is, it has not been submitted for the award of any academic degree, diploma, or certificate in any other university. All sources of materials that are used for this thesis have been duly acknowledged through citation.

Rahel Fitwi Gebrekirstos		08/09/2021
Name of Student	Signature	Date

RECOMMENDATION

We, the advisors of this thesis, hereby certify that we have read the revised version of the thesis entitled "Fuzzy Gain Scheduled Fractional-Order PID Temperature Control of a Continuous Stirred Tank Reactor Process" prepared under our guidance by Rahel Fitwi submitted in partial fulfillment of the requirements for the degree of Masters of Science in electrical power and control engineering (control). Therefore, we recommend the submission of the revised version of the thesis to the department following the applicable procedures.

Prof. Gang Gyoo Jin		08/09/2021
Advisor	Signature	Date
Mr. Minyamer Gelawe Wase (MSc.)		08/09/2021
Co-advisor	Signature	Date

APPROVAL SHEET

We, the advisors of this thesis entitled "Fuzzy Gain Scheduled Fractional-Order PID Temperature a Control of Continuous Stirred Tank Reactor Process" and developed by **Rahel Fitwi Gebrekirstos,** hereby certify that the recommendations and suggestions made by the board of examiners are appropriately incorporated into the final version of the thesis.

Prof. Gang Gyoo Jin		08/09/2021
Advisor	Signature	Date
Co-advisor	Signature	Date

We, the undersigned, members of the Board of Examiners of the thesis by **Rahel Fitwi** have read and evaluated the thesis entitled "Fuzzy Gain Scheduled Fractional-Order PID Temperature Control of Continuous Stirred Tank Reactor Process" and examined the candidate during open defense. This is, therefore, to certify that the thesis is accepted for partial fulfillment of the requirement of the degree of Master of Science in Electrical Power and Control Engineering (Control).

Chairperson	Signature	Date
Internal Examiner	Signature	Date
Dr Beteley Teka		Sept 08, 2021
External Examiner	Signature	Date

Finally, approval and acceptance of the thesis is contingent upon submission of its final copy to the Office of Postgraduate Studies (OPGS) through the Department Graduate Council (DGC) and School Graduate Committee (SGC).

Department Head	Signature	Date
School Dean	Signature	Date
Office of Postgraduate Studies, Dean	Signature	Date

ACKNOWLEDGEMENT

First of all, I would like to Praise and thanks GOD for his grace and blessing. My heartfelt thanks go to my advisor **Prof. Gang Gyoo Jin** for his unreserved support, constructive suggestions, motivation, enthusiastic encouragement, and insightful comments throughout thesis preparation. His patient guidance helped me all the time with the thesis preparation.

I am also very grateful to my co-advisor **Mr. Minyamer Gelawe Wase (MSc.)** for his lots of advice and continuous help equipping me with the necessary knowledge, regarding everything with the preparation of writing documentation.

I would moreover like to acknowledge **Dr. Tefera Terefe Ytayew** for his helpful advice and sharing of his knowledge.

My special thank also goes to Adama Science and technology university, the School of Electrical Engineering and Computing, and the department of Electrical Power and Control Engineering for give me a chance to study the master of science degree as a scholarship and funding me to perform this research thesis.

Finally, I thank my whole family and friends for their encouragement and all of the sacrifices that they have made up to this time.

TABLE OF CONTENTS

LIST OF TABLES

LIST OF FIGURES

LIST OF ACRONYMS

CSTR	Continuous Stirred Tank Reactor
CHR	Chien, Hrones and Reswich
CS	Cuckoo search
EOBL	Elite oppositional based learning
FIS	Fuzzy Inference System
FOPID	Fractional Order Proportional, Integral, and Derivative
FOPTD	First Order Plus Time Delay
GA	Genetic Algorithm
IAE	Integral Absolut Error
IAEU	Integral Absolut Error and Control signal
ISE	Integral Square Error
ITAE	Integral of Time Absolut Error
ITSE	Integral of Time Square Error
NARAM	Nonlinear Autoregressive Moving Average
PID	Proportional, Integral, and Derivative
PSO	Particles Swarm Optimization
SMS	State of matter search
T-S	Takagi Sugeno
ZN	Ziegler Nichols

ABSTRACT

CSTR is one of the most common reactors used for chemical production in all chemical industries, in which reactants continuously enter to the reactor while products are continuously leave from the reactor. CSTR is a highly nonlinear process exhibiting stable and unstable equilibrium points. In this regard, designing a single controller for stable and unstable regions is impossible. In this research work, fuzzy gain scheduling fractional-order PID (FOPID) temperature control of a CSTR process has been investigated. The mathematical modeling of the CSTR process based on mass and energy balance inside the reactor is done. Due to its nonlinearity and instability, the entire region divides into two regions. Two local FOPID controllers are designed for each region. The parameters of the FOPID controllers are tuned by a genetic algorithm (GA). In order to minimize the overshoot of the control signal the tuning of the controllers is done based on the integral absolute error and control input (IAEU). Then, a fuzzy gain scheduling method is used to smoothly select a local controller suitable for the current operating region. This is done based on the schedular variable (reactor temperature) and then it combined by the Tagaki-Sugno fuzzy model. The entire system including the controller design is implemented in MATLAB/Simulink. Also, the performance of the controller has been evaluated based on the setpoint tracking and disturbance rejection capabilities. The performance of the controller tuning is measured using an integral absolute error (IAE). A comparative analysis with two existing works (PID controller and adaptive nonlinear controller) is investigated. From the simulation result the proposed controller gives a settling time of 1.0232, overshoot 0%, in a 0.886 for setpoint tracking response. For the disturbance rejection, the proposed controller gives a settling time of 7.3426, overshoot 7.1%, and IAE of 0.0021 in a 0.886 setpoint tracking response, The simulation results have shown that, the proposed fuzzy gain scheduled FOPID controller outperformed the existing control systems.

Keywords: CSTR process, FOPID controller, Fuzzy gain scheduling, and Genetic Algorithm

CHAPTER ONE

INTRODUCTION

1.1 Background

In the development of technology, chemical reactors have a significant role for chemical industries in producing chemical products. A chemical reactor is an equipment unit used to produce different chemical products by using chemical transformation(reactions) of the raw materials into valuable chemical products at a certain production rate [1]. A chemical reaction is a process in which substances (reactants) are converted into another substance (product) to produce a new product with a new property [2]. This chemical reaction can be exothermic or endothermic according to types of the reaction in the chemical process. when the endothermic chemical reaction occurs, the energy is absorbed in the form of heat from the surrounding. When exothermic reactions occur, the energy is released from the system to the surrounding.

Different chemical reactors are used for industrial production based on their purpose in the production of chemical products includes a batch reactor, continuous tank stirred tank reactor, and plug flow tubular reactor [3]. All chemical reactors are anticipated to fulfill three fundamental requirements such as giving suitable contacting of reactant, permitting the reaction time for the formation of the desired product, and allowing the heat transfer capability required to maintain the range of specific temperature [4] [5]. To select, design, and operate a chemical reactor, it is necessary to identify the phenomena involved, understand how they affect the reactor operation, and express these effects in mathematical modeling.

Continuous stirred tank reactor (CSTR) is one of the most typically known chemical reactor. Chemical production mostly uses CSTR for plastic, syntactic material, chemical fibers. It's also used in the production of fuel, paint, pesticide, and so on [6]. It has two important roles which are used for the production of a chemical reaction. The first part is the internal feeding reacting element and the other one is a cooling element. The cooling elements are the outer part which has cooling pipes with different thicknesses and cross-sections. Cooling water is flowing through the cooling pipe to regulate the heat generated within the reactor. CSTR process in the industrial environment is shown in the Figure 1.1.

Figure 1.1 Continuous stirred tank reactor (CSTR) [7]

CSTR process exhibits highly nonlinear behavior due to variation of parameters like the concentration on the reactant and temperature of the reactor [8]. The heat generates in the reaction is caused by inlet concentration and inlet temperature. This leads rapid increase the temperature of the reactor. Due to this temperature control of the CSTR process is one of the critical issue problems in the chemical industries and others.

Most of the industries widely used PID controllers due to their simple structure and cost-effectiveness [9]. It is more suitable for a linear system than a nonlinear system. For highly nonlinear systems like the CSTR process, the PID controller may not achieve the required performance whenever the operating points are nonlinear.

Several techniques and algorithms have been proposed by researchers for the temperature control of the CSTR process. Among them are Ziegler Nichols-based PID (ZN-PID), Genetic Algorithm based PID (GA-PID), Fuzzy-PID, Fussy logic, and adaptive controllers have been widely used in the temperature control of the CSTR process.

In this research work, a fuzzy gain scheduling-based fractional order PID (FOPID) controller is proposed for the temperature control of the CSTR process. Since the CSTR process exhibits stability in one region and unstable in the other region, only one controller cannot be effective in controlling the process. Two local FOPID controllers are used one for the stable region and another for unstable region. Each controller is applied based on the temperature operating range. In order to select the proper controller fuzzy gain scheduling technique is used. Fuzzy gain scheduling method switches the controller automatically by selecting the proper controller on the current condition of the controlled variable. The overall system was designed mathematically and implemented in MATLAB/Simulink software tool.

1.2 Statement of the Problem

In the industrial process, a CSTR process that allows exothermic reaction is the most interesting system to study due to its potential safety problems (rapid increase in temperature). Since exothermic reaction releases the heat generated in the reactor, and the reactor's temperature increases so fast. This affects the formation of the product in case of quality and loss of the amount as well. It is also highly affecting the safety and lifetime of the reactor. Temperature of CSTR process should be controlled using an appropriate control mechanism to improve the above-mentioned problems and for the process reliability.

Several industrial processes used conventional PID controller to maintain temperature of the plant at the required level. However, since PID controller is a linear system control method and may not achieve good performance for the highly nonlinear system like CSTR process. It affects the overall performance of the process and reduce the amount of the product. Other nonlinear control system methods like Fractional Order PID (FOPID) controller are effective in case of minimizing the effect of disturbances and setpoint change problems. However, due to the nonlinear structure of the inlet and outlet temperatures a CSTR process exhibits two different regions. These are stable and unstable regions and can be distinguished based on the equilibrium points of the system. Designing a single controller in these two regions is difficult due to the stability problems. Therefore, in these research work two FOPID controllers using fuzzy gain scheduling technique is proposed. For tuning of the controller parameters genetic algorithm (GA) is used. The overall system simulation is conducted in MATLAB software tool.

1.3 Objective of the Study

1.3.1 General Objective

The general objective of this study is to design a fuzzy gain scheduled fractional-order PID controller using genetic algorithm optimization for the temperature control of a CSTR process.

1.3.2 Specific Objectives

The following points are the specific objectives:

- To design two local FOPID controllers for temperature control of the CSTR process based on their operating regions.
- To design fuzzy gain scheduling technique.
- To improve the dynamic performances of temperature for the proposed CSTR process based on genetic algorithm optimization.
- To justify the effectiveness of the proposed method by comparing it with the existing methods.

1.4 Scope of the Study

This research work focuses on the design and simulation of temperature control of CSTR using Fuzzy gain scheduling FOPID controller. It covers the mathematical modeling of the CSTR process based on the chemical reaction using material and energy balance model, designing of FOPID controller using GA tuning method, and implementation of fuzzy gain scheduling method.

1.5 Limitation of the Study

Since CSTR is found in different industries, every system has different operating conditions. In line with this, the operators in industries, they don't have any ideas how the CSTR process internally configured and they don't know about the entire process data. Only they operate and checking the minimum and maximum temperature ranges of the process. In this regard, it is difficult to get all the parameters of CSTR process data from the industries. The data that can't be get from the industries are taken from other related surveys. In addition, due to complexity it is limited to only temperature control of the process and controlling of the concentration reactant is not included.

1.6 Motivation of the Study

Knowing about process control theory is a very important concept for the control engineering research area. CSTR is one of the examples of the industrial process which can be used to learn different control systems. In practice, the CSTR process is very important especially in human daily life such as producing antidotes in medicine, food processing, water treatment, etc. To get these benefits, the process should be regulated with the appropriate controller. Therefore, this makes the research area focused on the CSTR process.

1.7 Significance of the Study

Any chemical industries need to have a high amount of production with better quality. To get such an advantage, they should use quality chemical reactors with better controls that can achieve their objective. This study allows the chemical reactor to be effective in its operation by reducing the heat generated on its surface. It enables chemical factories to avoid unnecessary loss or wastage of products and to deliver a good quality of products to the community at any time and place.

1.8 Thesis Organization

The thesis has been organized into five chapters.

Chapter-1: present the background of the study, statement of problems, the objective of the study, significance scope, motivation and limitation of the researcher.
Chapter-2: discuss the theoretical background and related works on the control systems of CSTR processes.
Chapter-3: described the methodology of following in this researcher's work.
Chapter-4: illustrates the controller design.
Chapter-5: presents the proposed results and discussions.
Finally, discussions of the conclusion and recommendation.

CHAPTER TWO

THEORETICAL BACKGROUND AND RELATED WORKS

2.1 Chemical Reactor Overview

Most industrials processes use chemical reactors to convert basic raw materials into products. Many materials used in clothing, housing, automobiles, appliances, construction, electronics, and healthcare come from processes that use chemical reactors. Chemical reactors are also important in the food processing and beverage industries that process agricultural products [10].

Since the entries chemical process is centered in a chemical reactor, the design of the chemical reactor is the most important factor that determines the economics of the entire process. Therefore, when designing the reactor, the designer must ensure that the product reaches the highest efficiency of the expected output product, produces the highest product output, and requires the least capital to pursue and operate[11]. The factors that affect the design of the reactor are reaction type, heat removal/addition, catalyst required, phases involved, temperature and pressure control methods, flow production capacity, residence time, contact/mixing between reactants[12].

Chemical reactors can be divided into batch reactors, continuous reactors, and semi-continuous reactors according to their operating modes [13]. A batch reactor is a tank in which a pump around the loop is used to agitate the reactants, a part of which is removed and recycled back to the reactor from the outside. The batch method is suitable for small production speeds and long reaction times.

In a continuous reactor, the reactants are added and the product is continuously removed at a constant mass flow rate. There are three types of continuous reactors: continuously stirred tank reactors (CSTR), plug flow reactors, or tubular reactors [13] [14]. CSTR is most commonly used in industrial processing, mainly for homogeneous liquid phase flow reactions that require continuous stirring. The plug flow reactor consists of a hollow tube or tube through which the reactants flow. Plug flow reactors are mainly used in liquid or gas phase systems. Semi-continuous reactors operate with continuous and batch inputs and outputs. In a semi-batch reactor, the chemical reactor is loaded into the reactor and the second chemical substance is slowly added, or the product produced by the phase change is continuously removed.

2.2 Continuous Stirred Tank Reactor (CSTR)

The Continuous Stirred Tank Reactor (CSTR) is a common chemical reactor in the chemical production process industry, in which the reactants are continuously fed into the reactor, while the products are continuously withdrawn from the reactor [14]. CSTR process operates under steady-state conditions with a perfect mix of reactants through the reactor.

The CSTR is composed of a tank equipped with a mixing motor, a cooling jacket, a stirrer, a baffle, a reaction vessel, and inlet and outlet pipes [15].The reactants are feed into the reactor through the feed line, and the agitator is used to mix the fluids in the reactor. The motor is used to rotate the stirrer to stir the reaction. The reactor is then thoroughly mixed and sent out through the outlet stream. Since the reaction is completely mixed, the flowing stream has the same concentration and temperature as the reactor fluid. Baffles are attached to the inner wall to promote mixing and increase heat transfer and possible chemical reaction rates. The cross-section diagram of CSTR process is shown in the Figure 2.1.

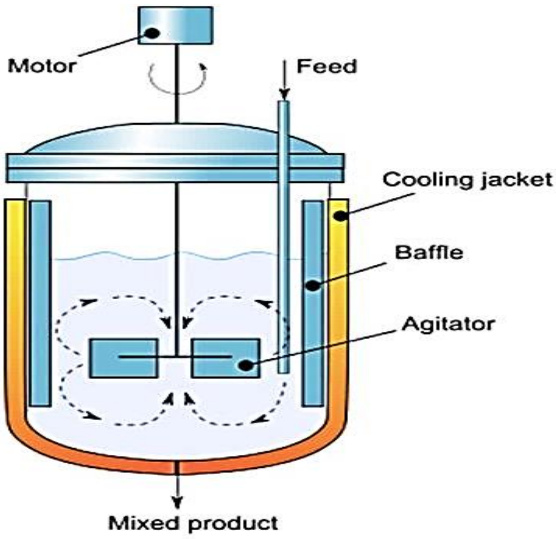

Figure 2.1 CSTR cross-section diagram [15]

The jacket surrounding the reactor is used for cooling or heating, depending on the type of chemical reaction that occurs in the reaction, which is exothermic or endothermic, respectively [16]. In this study, the exothermic CSTR process was used. For exothermic reactions, a cooling jacket is used to remove excess heat to maintain the temperature of the reactor. The jacket has a feed flow and an outlet flow [17]. It is assumed that the jacket is completely mixed and its temperature is lower than the temperature of the reactor. Therefore, the temperature of the reactor is controlled by manipulating the coolant temperature.

2.3 Existing Works on Temperature Control of CSTR

2.3.1 PID Control

The PID controller has become the most widely used controller in the chemical process industry because of its simplicity and cost-effectiveness [18]. It consists of three parameters which are proportional, integral, and derivative terms. The combination of these parameters provides a control strategy for process control. Its structure is shown in Figure 2.2.

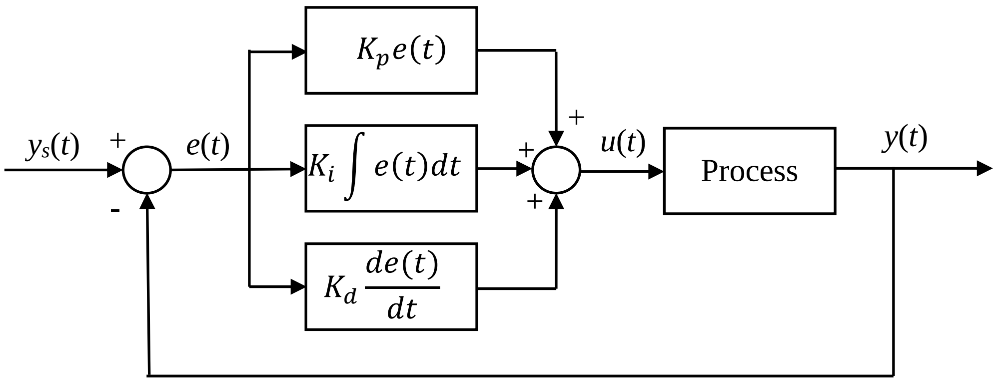

Figure 2.2 Structure of the PID controller [19]

The time-domain equation of PID controller is given by [20]

$$u(t) = K_P e(t) + K_i \int_0^t e(t) + K_d \frac{de(t)}{dt} \tag{2.1}$$

where $u(t)$ denotes the control input, $e(t)$ the error between the setpoint $y_s(t)$ and the output $y(t)$; K_p, K_i, and K_d the proportional gain, the integral gain, and the derivative gain, respectively. The frequency-domain form can be obtained by taking the Laplace to transform [20],

$$C(s) = K_p + \frac{K_i}{s} + K_d s \tag{2.2}$$

Many tuning methods for PID controllers have been proposed, such as the Ziegler-Nichols method, CHR method, Cochen and Coon method [21].

The CHR method is a modification of the Ziegler-Nichols open-loop method. This method recommends using the fastest response without overshoot or the fastest response with 20% overshoot as design criteria. It also made the different tuning methods of setpoint tracking and disturbance rejection. To adjust the controller according to the CHR method, the parameters of the first-order plus the time delay (FOPTD) model are determined in the same way as the Ziegler-Nichols method. [21].

The first-order plus time delay model is given in the following Equation.

$$G(s) = \frac{K}{1+Ts} e^{-Ls} \tag{2.3}$$

Given K, T, and L, the PID controller parameters can be determined from Table 2.1 and Table 2.2 [21].

Table 2.1 CHR tuning method of the PID controller for setpoint tracking.

Controller parameter	With 0% overshoot	With 20% overshoot
K_p	$0.6/K$	$0.95L/KT$
T_i	T	$1.4T$
T_d	$0.5L$	$0.47L$

Table 2.2 CHR tuning method of the PID controller for for disturbance rejection.

Controller parameter	With 0% overshoot	With 20% overshoot
K_p	$0.95L/KT$	$1.2\ L/KT$
T_i	$2.4L$	$2L$
T_d	$0.42L$	$0.42L$

2.3.2 Adaptive Control

Chen and Peng proposed an adaptive controller with input constraints for the CSTR process [22]. First, the bounded nonlinear controller whose output range is designed to fit the input constraint bounds is proposed as the process feedback controller. then the adaptive algorithm is derived based on the Lyapunov stability theorem that enables the bounded nonlinear controller to learn to control plant by observing the process output errors. Figure 2.3 depicts the block diagram of the adaptive learning algorithm.

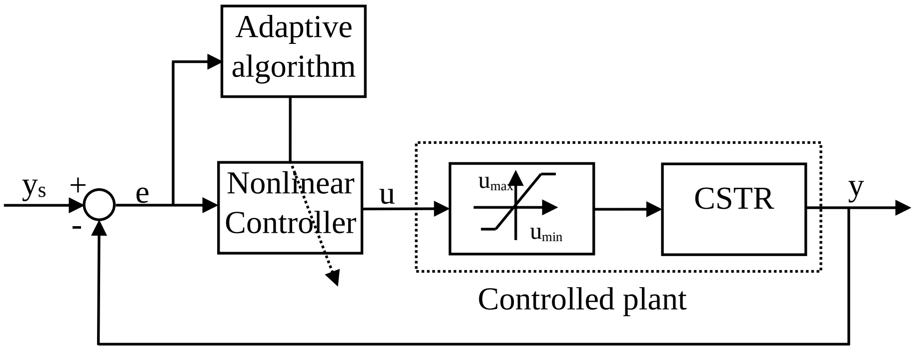

Figure 2.3 Block diagram of adaptive control system [22].

The control input bounded by saturation, u_{max} and u_{min} is given by the following equation [22].

$$u(t) = \frac{1}{2}[(1+\tilde{u}(t))u_{\max} + (1-\tilde{u}(t))u_{\min})] \tag{2.4}$$

where, $\tilde{u}(t)$ is the hyperbolic tangent and is given as follows:

$$\tilde{u}(t) = \frac{1-\exp[-be(t)-\theta]}{1+\exp[-be(t)-\theta]} \tag{2.5}$$

where, *e(t)* is the error between the setpoint and the output; *b* a slope (gain factor), and θ a bias (threshold).

Equation (2.5), $\tilde{u}(t)$ has two adjustment parameters, *b* and θ. Since the magnitude and sign of *b* is sensitive to the characteristics of the controller, *b* is fixed. Only the bias θ is adaptively adjusted by the adaptation algorithm. The algorithm is given in the following equation [22].

$$\dot{\theta}(t) = \eta b e(t)(1-\tilde{u}(t))(1+\tilde{u}(t) sign\left(\frac{\partial y}{\partial t}\right) \tag{2.6}$$

where, $\eta > 0$ is the rating rate and $sign(\partial y / \partial t)$ is obtained from the step response or the physical characteristics of the control object. By doing this, the algorithm continuously adjusts the parameters of the controller with the error between the setpoint and the output.

2.4 Related Works

The idea of temperature control for a CSTR process is not new and it has been reported on several research papers by using different control algorithms. Most of the works are implemented based on a PID controller. PID controller is the simplest method for linear systems. In some cases, it has been also implemented for nonlinear systems like controlling the temperature of CSTR. In this section, the closely related works are discussed based on the performance comparison parameters criteria like settling time, overshoot, and steady-state error. The methods, merits, and demerits are also discussed.

Temperature control of the CSTR process using a PID controller based on ZN tuning was implemented in the literature [23]. The authors used a jacketed temperature as the manipulated variable for the process. The performance of the controller was analyzed based on the constant setpoint tracking and disturbance rejection capabilities. The result shows that the system has a high overshoot (13.33 %). To reduce the overshoot, they considered the two degrees of freedom analysis, and the overshoot is reduced and it becomes 0%. However, this study focused on the linear region and stable ranges of the plant under constant setpoint conditions. This may cause difficulties in controlling the temperature of the plant whenever the operating conditions are nonlinear. research works focused on the stable and linear region of the system with a fixed setpoint.

A genetic algorithm tuned PID controller for the temperature control of the CSTR process was performed in [24]. For comparison purposes, the authors implemented the PID controller based on ZN tuning. The performance comparison analysis has been formulated based on the dynamic performance parameters like rising time (t_r), overshoot ($M_{p\%}$), peak time (t_p), and settling time (t_s) as shown in Table 2.3.

Table 2.3 Comparative analysis between PID-ZN method and GA-PID.

Controller methods	t_r (s)	M_p (%)	t_p (s)	t_s (s)
PID-ZN	0.1600	25.786	0.3550	1.5875
PID-GA	0.0600	12.667	0.1550	0.3279

As it can be seen in Table 2.3, in all aspects the GA-PID controller outperformed the ZN-PID controller. Even though the GA-PID controller result shows good results, it can be further improved. In addition, the system stability and the input/output nonlinearity conditions were not checked. Moreover, the authors were focused only on a fixed setpoint tracking performance analysis without showing the disturbance rejection capabilities and variable setpoint conditions. This may cause integral windup whenever the conditions are changed.

The authors in [25] developed a temperature control CSTR process based on the fuzzy-PID controller. Mamdani type FIS was considered for the implementations of fuzzy logic controllers. Its performance analysis has been carried out based on the constant setpoint tracking response. The result shows that the proposed controller has good performance than the conventional PID controller. However, the system is usually process parameter-dependent and sometimes it will become unstable and nonlinear. In this regard, the fuzzy controller may not tune the PID controller gains exactly and it will be out of range.

A comparative study of ZN-PID, Fuzzy-PID, and Nonlinear Autoregressive Moving Average (NARAM) based PID controllers were presented in the literature [26]. An offline training of a neural network was implemented for tuning of the PID controller gains in case of the NARAM-PID controller. The same constant reference temperature of 100℃ was applied for all methods. The result shows that the ZN-PID controller has poor performance than the other two methods. A NARAM-PID controller has less settling time as compared to a fuzzy-PID controller. But, the overshoot in the case of the fuzzy-PID controller is less. However, due to the variation of inlet temperature and concentration, usually the system has external disturbances. Due to the process production capacity sometimes the setpoint might be variable. Based on this, the proposed controller in this study may not achieve the required performance.

In a similar manner, a comparative study of temperature control for the CSTR process using ZN-PID, GA-PID, and PSO-PID was performed in the literature [27]. The comparative analysis has been done based on the setpoint and disturbance rejection conditions. From the result, the PSO tuned PID controller has better performance parameter results than the other two techniques. However, this doesn't mean that it has better results in general. It's overshoot for setpoint tracking results 12.6140% and overshoot for the disturbance rejection results 15.241%. This can be improved further to a certain recommended level of the process.

Optimal FOPID controller for CSTR temperature control using hybrid heuristic algorithm is designed in literature [28]. The FOPID controller parameter is tuned using hybrid of three algorithm (CSMS-EOBL), Cuckoo search (CS), State of matter search (SMS), and Elite oppositional based learning (EOBL). CSMSEOBL based FOPID is compared with SMS-FOPID, CS-FOPID, and PSO-FOPID. The result of the CSMSEOBL has been shown least settling time and minimum overshoot from the others. However, the analysis of the nonlinearity and stability problems is not discussed. Inline with this the effect of the external and disturbance effects was not discussed to check the controller performance.

In general, most of the reviewed literatures in this section was analyzed based on the constant setpoint tracking conditions. Besides the system is nonlinear and unstable in some regions within the operating range of the plant. In some cases, the results are also poor and can be improved further by applying advanced controllers.

Hence depending on the process production capacity usually the setpoint is variable. Also, the CSTR process is always dependent on the inlet temperature and concentration. This may lead to external disturbance in the concentration as well as the temperature of the plant. A PID controller is effective in a fixed operating range. However, the plant exhibits highly nonlinear and unstable ranges in the input and output relations. As a result, the PID controller may not achieve the required performance whenever there are instability and nonlinearity problems.

In this research study, a fractional-order PID (FOPID) controller is proposed to mitigate the non-linearity problems of the plant. However, due to the stable and unstable regions of the plant applying a single controller is inefficient. For this, depending on the operating ranges of the stable and unstable regions, two local FOPID controllers are implemented. To switch these controllers depending on the current state of the controlled variable fuzzy logic controller is used. A genetic algorithm is used to tune the two local FOPID controllers individually within their operating ranges. In general, the result of this proposed study shows a better transient and steady-state dynamic performance of the plant in all aspects.

CHAPTER THREE

MODELING OF CSTR PROCESS

This chapter deals with the mathematical modeling of a CSTR process based on data collection and analysis. Then nonlinearity behavior of the system is checked using the open-loop system and a phase plane diagram is drawn to check the stability of the system.

3.1 Methodologies

The method used in this study to accomplish the required task is shown in Figure 3.1.

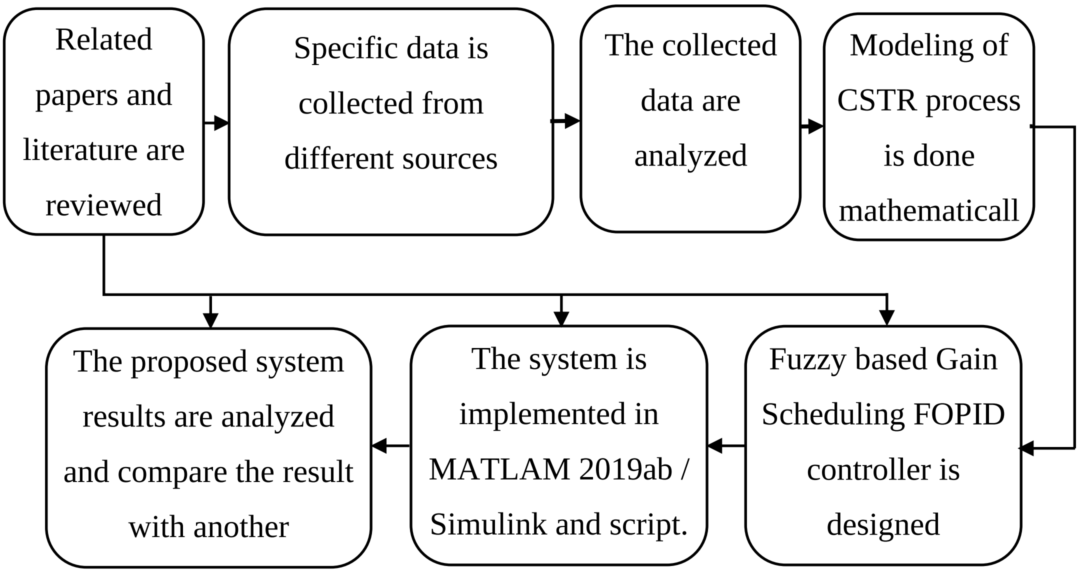

Figure 3.1 Block diagram of the proposed methodology

The closely related papers and literature are reviewed. Then the necessary data used throughout this research work is collected and analyzed. The mathematical modeling of the CSTR process is developed and the stability analysis is also done based on the equilibrium state equations. Fuzzy gain scheduling of the FOPID controller is designed to control the temperature of the CSTR process. Then the system is simulated on MATLAB/Simulink and the proposed system result is analyzed by compared with the conventional methods. Finally, the research work is concluded and recommended for the future.

3.2 Modeling of CSTR Process

CSTR process with A-B first-order a perfectly mixed irreversible exothermic reaction is shown in Figure 3.2.

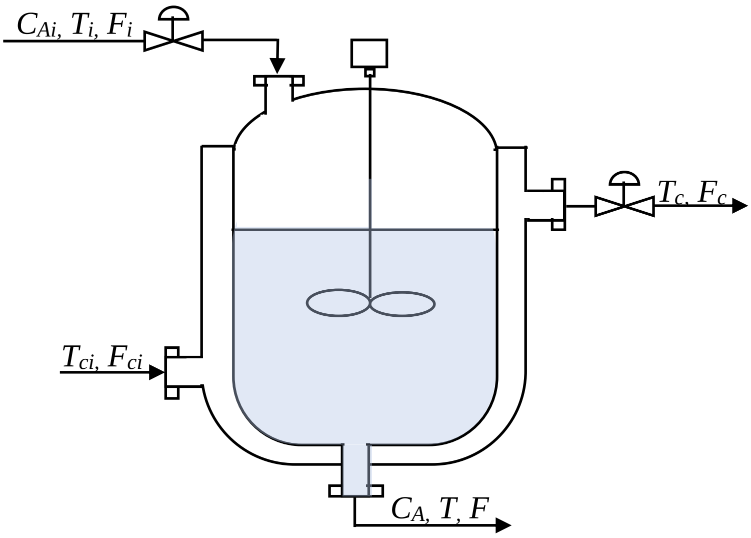

Figure 3.2 CSTR process [29]

A is the reactant in the reactor and B is the product from the reactor. in the feed stream, there is an inlet temperature, inlet flow rate, and inlet concentration of reactant. in the exit stream, there is outlet temperature, outlet flowrate, and outlet concentration [30]. In the cooling jacketed feed stream, there is an inlet coolant temperature and inlet flowrate and on exited stream, there is outlet coolant temperature and outlet flowrate. Since the fluid inside the reactor is perfectly mixed, the temperature and concentration at which the reaction takes place are the same as the temperature and concentration of the exited stream [17][30]. The dynamic model of the CSTR process is mathematically represented by using a conservation equation that includes mass and energy balance equations [31].

To develop mathematical models, some assumption is considered [31]:

- The reaction is perfectly mixed which indicated the temperature concentration of the reactor are the same in everywhere, the liquid density, heat capacity and the Volume are constant
- There is no heat loss from the reactor to the surrounding, coolant is perfectly mixed which indicated no energy balance for the coolant.

- The momentum of the CSTR is negligible that doesn't have change under any operating conditions.

Also, for convenience, time is denoted by t' to distinguish it from dimensionless time t discussed in Subsection 3.2.4.

The reaction rate, r is given by [32]

$$r = kC_A \tag{3.1}$$

where r is the mole of A reacted per unit time, per unit volume, C_A is the concentration of A (mole per unit volume), and k is the rate constant (units of reciprocal time).

The rate constant has an Arrhenius Temperature dependence [32].

$$k = k_0 \exp(E / RT) \tag{3.2}$$

where k_0 is the frequency factor, E is the activation energy, and R is the gas constant.

The mathematical modeling of the CSTR process is developed using total mass balance, component mass balance, and energy balance.

3.2.1 Total mass Balance Equation

The total mass balance equation is given by the principle of conservation mass. The general mass balance equation of any system is as follows [29] [33].

$$\begin{pmatrix}\text{Rate of mass}\\ \text{accumulation}\end{pmatrix} = \begin{pmatrix}\text{Mass flow}\\ \text{input}\end{pmatrix} - \begin{pmatrix}\text{Mass flow}\\ \text{output}\end{pmatrix}$$

$$\frac{dm}{dt'} = F_{mi} - F_{mo} \tag{3.3}$$

where dm/dt' is the time rate of change of mass inside the system: F_{mi}, F_{mo} are mass flow in and mass flow out of the system respectively.

$$m = Vp,\ F_{mi} = F_i p,\ F_{mo} = Fp \tag{3.4}$$

Substitute Equation (3.4) to (3.3)

$$\frac{d(Vp)}{dt'} = F_i p_i - Fp \tag{3.5}$$

where F_i, F is the flowrate of inlet and outlet stream; P_i, P is densities of inlet and outlet stream; V is the volume of the reactor.

Since density remain constant,

$$p_i = p, \ \frac{d(Vp)}{dt'} = 0 \tag{3.6}$$

Then substitute Equation (3.6) to (3.5)

$$\begin{aligned} 0 &= p(F_i - F) \\ 0 &= F_i - F \\ F_i &= F \end{aligned} \tag{3.7}$$

Therefore, Equation (3.7) is shown that the system inlet and outlet flowrate are the same.

3.2.2 Component Balance Equation

Component mass balance equation of CSTR process for the reactant A is given as follows [33].

$$\begin{pmatrix} \text{Rate of mole accumulation} \\ \text{of component A} \end{pmatrix} = \begin{pmatrix} \text{Mole component} \\ \text{flow input} \end{pmatrix} - \begin{pmatrix} \text{Mole component} \\ \text{flow output} \end{pmatrix} + \begin{pmatrix} \text{Rate} \\ \text{Generation} \end{pmatrix}$$

$$\frac{dn_A}{dt'} = F_{Ani} - F_{Ano} + G_A \tag{3.8}$$

$$\frac{dn_A}{dt'} = \frac{d(VC_A)}{dt'}, \ F_{Ani} = F_i C_{Ai}, \ F_{Ano} = FC_A, \ G_A = -VkC_A \tag{3.9}$$

Then substitute Equation (3.9) to (3.8)

$$\frac{dVC_A}{dt'} = F_i C_{Ai} - FC_A - VkC_A \tag{3.10}$$

where C_{Ai}, C_A is the is the concentration of reactor A of inlet and outlet stream; F_i, F is flowrate of inlet and outlet stream; V is the volume of the system; k is rate constant.

The minus sign in the rate formation comes from the fact that *A* is being consumed, not produced. The units of all these terms must be the same mole of *A* per unit time. Therefore, the unit of VkC_A *must* have these units and the units of *k* in this system are min^{-1}.

Since the volume of the system is constant, Equation (3.10) can be written as

$$V\frac{dC_A}{dt'} = F_iC_{Ai} - FC_A - VkC_A \tag{3.11}$$

Then divide both sides by *V* and substitute Equation (3.7) to (3.11)

$$\frac{dC_A}{dt'} = \frac{F}{V}(C_{Ai} - C_A) - kC_A \tag{3.12}$$

Substitute Equation (3.2) to (3.12).

$$\frac{dC_A}{dt'} = \frac{F}{V}(C_{Ai} - C_A) - k_0e^{-E/RT}C_A \tag{3.13}$$

where k_0 is the first-order rate constant; *E* is Activation energy; *R* is universal ideal constant; *T* Arrhenius temperature. Therefore Equation (3.13) is shown the component balance equation of the CSTR process.

3.2.3 Energy Balance Equation

The general energy balance equation for the CSTR process is given by the conservation of energy. Based on these the Equation is given as follow [33].

$$\begin{pmatrix}\text{Rate of Energy}\\ \text{accumulation}\end{pmatrix} = \begin{pmatrix}\text{Rate of energry}\\ \text{input}\end{pmatrix} - \begin{pmatrix}\text{Rate of energy}\\ \text{output}\end{pmatrix} - \begin{pmatrix}\text{Rate of energy}\\ \text{Removed by coolant}\end{pmatrix} + \begin{pmatrix}\text{Rate energy added}\\ \text{by exothermic rection}\end{pmatrix}$$

$$\frac{d(Vpc_pT)}{dt'} = F_ip_ic_{p_i}T_i - Fpc_pT - hA(T - T_c) + (-\Delta H)Vr \tag{3.14}$$

where, T_i, *T* is temperature inlet and outlet stream; T_c is coolant temperature; ΔH is heat reaction; C_p is specific heat capacity; *hA* heat transfer.

Since volume, density and specific heat capacity is constant, Equation (3.14) then become

$$Vpc_p \frac{dT}{dt'} = FpC_p (T_i - T) - hA(T - T_c) + (-\Delta H)Vr \tag{3.15}$$

Then Divide Equation (3.15) both sides by VpC_p

$$\frac{dT}{dt'} = \frac{F}{V}(T_i - T) - \frac{hA}{VpC_p}(T - Tc) + \frac{(-\Delta H)}{pC_p} r \tag{3.16}$$

Substitute Equation (3.1) and (3.2) to Equation (3.16)

$$\frac{dT}{dt'} = F(T_i - T) - \frac{hA}{Vpc_p}(T - Tc) + \frac{(-\Delta H)}{pc_p} k_0 e^{-E/RT} C_A \tag{3.17}$$

Therefore, the general equation for the CSTR process is[33] [34] :

$$\frac{d(C_A)}{dt'} = \frac{F}{V}(C_{Ai} - C_A) - k_0 \exp(-E / RT) C_A \tag{3.18a}$$

$$\frac{dT}{dt'} = F(T_i - T) - \frac{hA}{Vpc_p}(T - Tc) + \frac{(-\Delta H)}{pc_p} k_0 e^{-E/RT} C_A \tag{3.18b}$$

3.2.4 Dimensionlessness of the Process Parameters

As it can be seen in Equation (3.18), the CSTR model equations inherit highly nonlinear elements with many parameters. By writing such complex equations in dimensionless form, it can make the problem simpler and treat the variables without physical dimension. First, to simplify the differential equations resulting from material and energy balances of the system, several dimensionless quantities are defined and the inputs, disturbances, and outputs to the system are also made to be dimensionless.

The nonlinear equation of the CSTR process can be put dimensionless by defining new variables[33] [35].

Let the dimensionless concentration and temperature be;

$$x_1 = \frac{(C_{Ai0} - C_A)}{C_{Aio}}$$
$$x_2 = \frac{(T - T_{io})}{T_{io}}\gamma \tag{3.19}$$

where x_1 and x_2 are dimensionless concentration and temperature of the reactor; the subscript i and o are representing the inlet feed values and the reference value respectively.

$$u = \frac{(T - T_{co})}{T_{io}},$$
$$\mathrm{t} = t' \frac{F}{V} \tag{3.20}$$

where u is the dimensionless coolant temperature, and t is dimensionless.

$$D_a = k_0 \, \mathrm{e}^{-\gamma} \frac{V}{F},$$
$$H = \frac{(-\Delta H) C_{Ai0} \gamma}{\rho C_\rho T_{i0}} \tag{3.21}$$

where D_a is Damkohler Number and H is the heat of reaction.

$$\beta = \frac{hA}{F_c \rho_c C_{\rho c}},$$
$$\gamma = \frac{E}{RT_{io}} \tag{3.22}$$

where β and γ is heat transfer coefficient and the ratio of activation energy to average kinetic energy.

$$d_1 = \frac{(C_{Ai} - C_{Aio})}{C_{Aio}},$$
$$d_2 = \frac{(T_i - T_{io})}{T_{io}}\gamma \tag{3.23}$$

where d_1 and d_2 are dimensionless feed temperature and concentration disturbance.

Thus, the CSTR model becomes [35]

$$\dot{x}_1 = -x_1 + D_a (1 - x_1) \exp\left(\frac{x_2}{1 + x_2 / \gamma}\right) + d_1 \tag{3.24a}$$

$$\dot{x}_2 = -(1+\beta)x_2 + HD_a(1-x_1)\exp(\frac{x_2}{1+x_2/\gamma}) + \beta u + d_2 \quad (3.24b)$$

$$y = x_2 \quad (3.24c)$$

Therefore, Equation (3.24) is the dimensionless dynamic model of the CSTR process [35]. The summary of variables used for the mathematical modeling of the CSTR process with their value is listed in Table 3.1.

Table 3.1 CSTR dynamic model parameter with their value [35] [36].

Parameter	Description	Value	Unit
$\gamma=E/RT_{io}$	Dimensionless activation Energy	20	-
$D_a=V/Fk_0e^{-\gamma}$	Damkohler Number	0.072	-
$\beta=hA/F_cP_cC_{pc}$	Dimensionless cooling rate	0.3	-
$H=-\Delta HC_{Aio}\gamma/PC_pT_{io}$	Dimensionless heat of reaction	8	-
C_{Aio}	Nominal feed concentration	3.526	$k\ mol/m^3$
T_{io}	Nominal Feed temperature	295	K
V	Volume of reactor	1	m^3
F	Steady state flow rate	1	m^3/min
F_c	Coolant flow rate	1.413	m^3/min
E	Activation Energy	69815	$kJ/k\ mol$
R	Universal idea gas constant	11.833	$kJ/k\ mol$
C_p	Inlet and outlet stream heat capacity	3.13	$kJ/kg\ K$
C_{pc}	Cooing water heat capacity	2.79	$kJ/\ kg\ K$
P	Inlet and outlet stream of Density	800	Kg/m^3
P_c	Cooling water density	1000	Kg/m^3
k_0	First order reaction rate constant	$3.4931\text{x}10^7$	min^{-1}
A	Area of heat transfer	23.22	m^2
h	Heat transfer	51.08	$KJ/min\ m^2\ K$

3.3 Analysis of Open-loop System

As can be expected from Equation (3.24), CSTR is highly non-linear, so it is a system that shows very different dynamic characteristics depending on the operating point and is also sensitive to parameter changes.

3.3.1 Equilibrium States

To find the equilibrium point, the system should be solved for the state variables while equating the derivatives of the state variable, the input, and disturbances to zero. From Equation (3.24), letting $\dot{x}_1 = 0,\ \dot{x}_2 = 0$, *u*= 0, *d*1=0, and *d*2= 0 yields,

$$\begin{aligned} -x_1 + D_a(1-x_1)\exp\left(\frac{x_2}{1+x_2/\gamma}\right) &= 0 \\ x_1 &= D_a(1-x_1)\exp\left(\frac{x_2}{1+x_2/\gamma}\right) \end{aligned} \tag{3.25a}$$

$$\begin{aligned} -(1+\beta)x_2 + HD_a(1-x_1)\exp\left(\frac{x_2}{1+x_2/\gamma}\right) &= 0 \\ \frac{(1+\beta)x_2}{H} &= D_a(1-x_1)\exp\left(\frac{x_2}{1+x_2/\gamma}\right) \end{aligned} \tag{3.25b}$$

Then rewrite Equation (3.25a)

$$-x_1 - D_a\exp\left(\frac{x_2}{1+x_2/\gamma}\right) - x_1 D_a\exp\left(\frac{x_2}{1+x_2/\gamma}\right) = 0$$

$$-x_1 - x_1 D_a\exp\left(\frac{x_2}{1+x_2/\gamma}\right) = -D_a\exp\left(\frac{x_2}{1+x_2/\gamma}\right)$$

$$-x_1\left(1 + D_a\exp\left(\frac{x_2}{1+x_2/\gamma}\right)\right) = -D_a\exp\left(\frac{x_2}{1+x_2/\gamma}\right)$$

$$x_1 = \frac{D_a\exp\left(\frac{x_2}{1+x_2/\gamma}\right)}{\left(1 + D_a\exp\left(\frac{x_2}{1+x_2/\gamma}\right)\right)} \tag{3.26}$$

Or Substituting Equation (3.25b) to Equation (3.25a), we get the following equations

$$x_1 = \frac{(1+\beta)}{H}x_2 \tag{3.27}$$

Substituting Equation (3.27) to (3.25b) gives

$$f(x_2) = -\frac{(1+\beta)}{H}x_2 + D_a\left(1 - \frac{1+\beta}{H}x_2\right)\exp\left(\frac{x_2}{1+x_2/\gamma}\right) = 0 \tag{3.28}$$

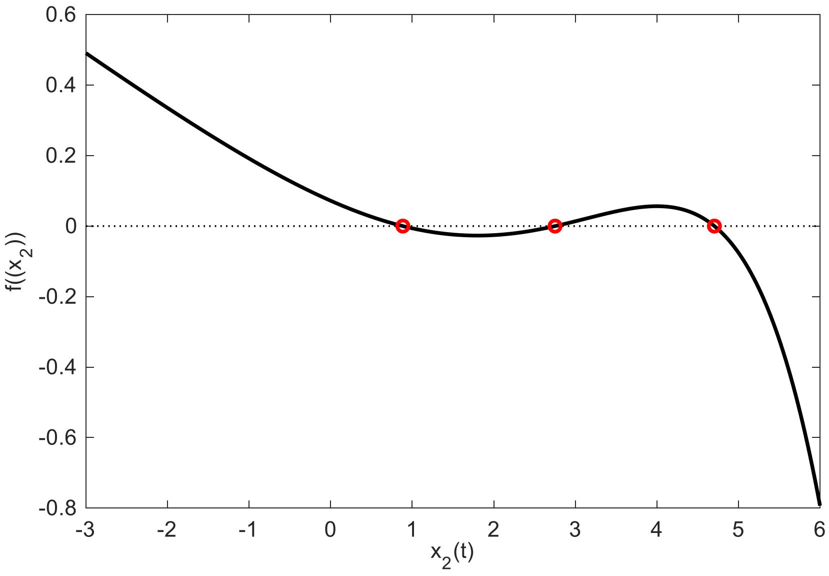

Figure 3.3 Curve of $f(x_2)$

Equation (3.28) is a nonlinear function to x_2 and its solution can be found using a root finding method. Figure 3.3 shows the curve of $f(x_2)$ with typical parameter values of D_a= 0.072, H= 8, β= 0.3, and γ= 20. As it can be seen in the figure that there exist three solutions.

If x_2 is obtained, x_1 can be easily calculated by Equation (3.27). These can be done by the MATLAB Fzero function. The MATLAB Fzero function is used for the nonlinear equation to solve for zero of a function of a single variable.

Therefore, three equilibrium points of the CSTR system can be found as:

$$\boldsymbol{x}_a = [0.1446, 0.8860]^T \quad (3.29a)$$

$$\boldsymbol{x}_b = [0.4472, 2.7517]^T \quad (3.29b)$$

$$\boldsymbol{x}_c = [0.7646, 4.7050]^T \quad (3.29c)$$

Figure 3.4 depicts the x_1-x_2 phase diagram of the homogeneous CSTR process in Equation (3.24). Different initial data is taken from x_1 and x_2 to draw the phase diagram. As it can be seen from the phasor diagram, some arbitrary points based on each equilibrium points has been checked and their wave forms enter the first equilibrium point $[0.1446, 0.8860]^T$ and others are entering the third equilibrium point $[0.7646, 4.7050]^T$. However, there is no points approaching the second equilibrium point $[0.4472, 2.7517]^T$. This indicates the second equilibrium point is unstable but the first and third equilibrium points are stable.

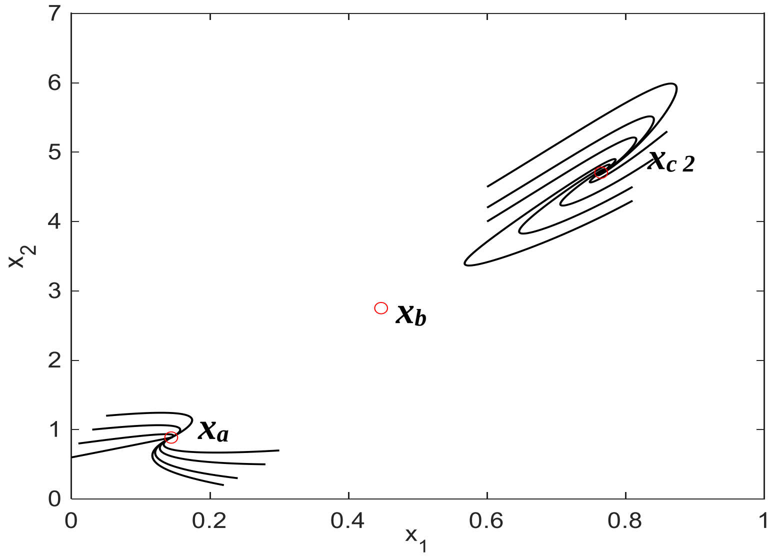

Figure 3.4 Phase diagram and equilibrium points

3.3.2 Open-loop response

The nonlinear behavior of the CSTR process can be tested by an open-loop response. Step-type different coolant temperature as the control input is applied to Equation (3.24) and then responses are plotted.

Figure 3.5 shows the open-loop response for the temperature of CSTR response in a given graph. As it can be seen from the graph when the control input increases the nonlinearity of the system is increased. This shows that the CSTR process is a highly nonlinear system.

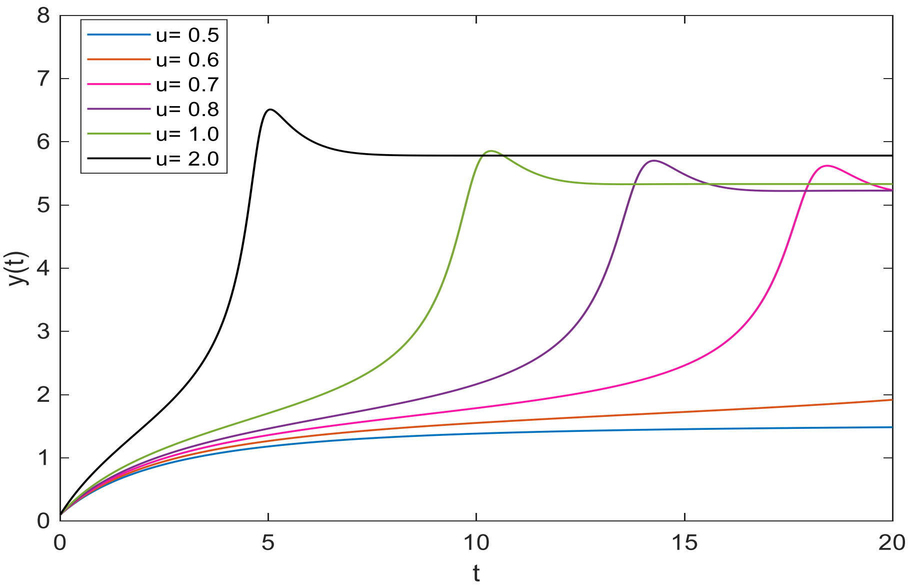

Figure 3.5 Open-loop responses of the CSTR process for different control inputs

3.3.3 Steady-state Analysis

To analyze the steady-state of the CSTR process without disturbances for different control inputs, Equation (3.24b) can be rewritten as:

$$-(1+\beta)x_2 - \Delta H x_1 + \beta u = 0 \tag{3.30}$$

Substitute Equation (3.25a) to (3.30)

$$-(1+\beta)x_2 + HD_a(1-x_1)\exp(x_2/1+x_2/\gamma) + \beta u = 0 \tag{3.31}$$

Then the steady-state control input equation is as follows

$$u = \frac{(1+\beta)x_2 + D_a H(1-x_1)\exp(x_2/1+x_2/\gamma)}{\beta} \tag{3.32}$$

The relationship of x_1(t) and $x_2(t)$ vs $u(t)$ in the steady-state is shown in Figure 3.6. x_1(t) and $x_2(t)$ are obtained while changing $u(t)$ from -5 to 5. The red dots show the three equilibrium points.

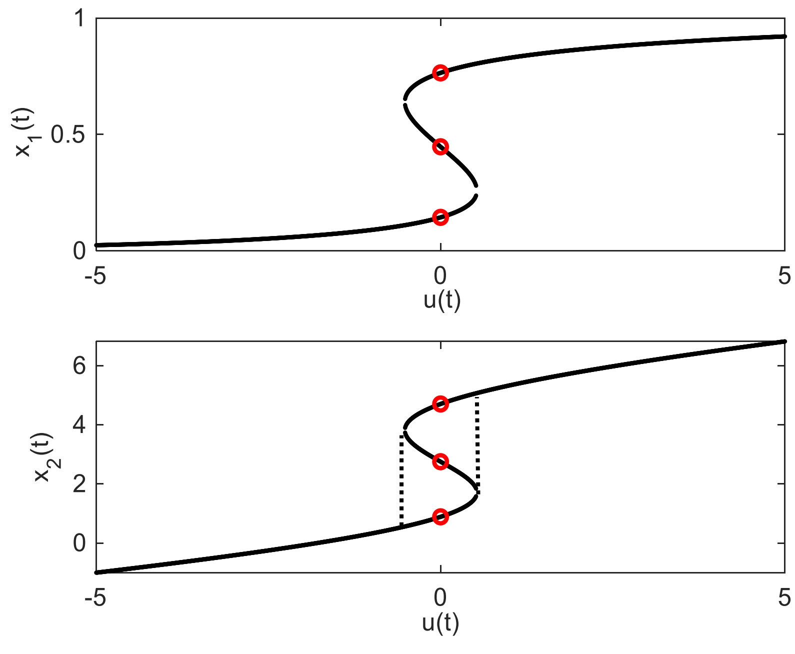

Figure 3.6 Steady-state values of the CSTR process for different control input

The graph shows the characteristics similar to nonlinearity hysteresis for $u(t)$ between -0.5 and 0. As shown in the figure, $x_1(t)$ and $x_2(t)$ increase smoothly as $u(t)$ increases except that they increase abruptly around $u(t)$= 0.5 and on the contrary, $x_1(t)$ and $x_2(t)$ show smoothly decreasing characteristics as $u(t)$ decreases except abrupt decrease around $u(t)$= -0.5.

This nonlinear dynamic characteristic shows that there is a limitation to control over the overall operating points with a conventional fixed-parameter controller. For this study, the working operating range of the CSTR process is up to the second region. The simulation data of this specific CSTR process operating temperature is not beyond the second region.

CHAPTER FOUR

DESIGN OF A FUZZY GAIN SCHEDULED FOPID CONTROLLER

In this chapter, a FOPID controller using fuzzy gain scheduling is designed and deal with how to optimally tune the parameters of the FOPID controller.

4.1 Proposed Control System

As mentioned earlier, CSTR exhibits highly nonlinear properties with several equilibrium points and also shows different dynamic characteristics depending on operating points. This makes the system difficult to control. To overcome such difficulties, several techniques have been proposed. In this study, a FOPID control system incorporating a fuzzy gain scheduling scheme is proposed. The overall system consists of four components: FOPID controller as a local controller, fuzzy gain scheduler, input saturation, and the CSTR process as a controlled object. Figure 4.1 depicts the overall block diagram

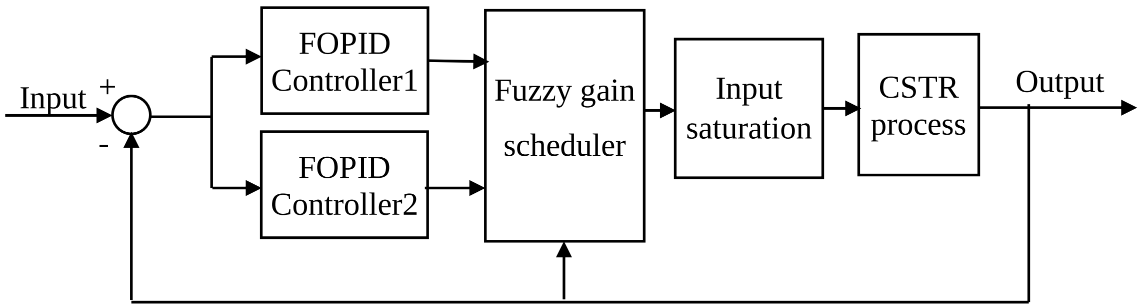

Figure 4.1 Structure of the proposed CSTR temperature control system

4.2 Design of a FOPID Controller

The PID controller has been still widely used, accounting for more than 90% of control loops used in industrial processes such as chemical processes, power plant stations, electric drives, and so on. However, since most of the industrial processes have their structural complexity, uncertainty, and nonlinearity behavior, it is difficult to control using the PID controller [37]. In order to reduce such problems, the PID controller was modified by Podlubny in 1997 [38] , which is known as fractional-order PID (FOPID) controller. A fractional-order controller is designed based on the principle that the classical integer of I-term and D-term in PID controller can be generalized into non-integer order operation. Unlike the conventional PID controller, it has five parameters; proportional gain, integral gain, derivative gain, integral, and derivative orders [38].

The graphical representation of PID points and the FOPID plane using an integrator and derivative order in the horizontal and vertical axis is shown in Figure 4.2. If $\lambda=\mu=1$, then PID controller is obtained, if $\lambda=1$and $\mu=0$, then it became PI controller and if $\lambda=\mu=0$, then PD controller is obtained [39].

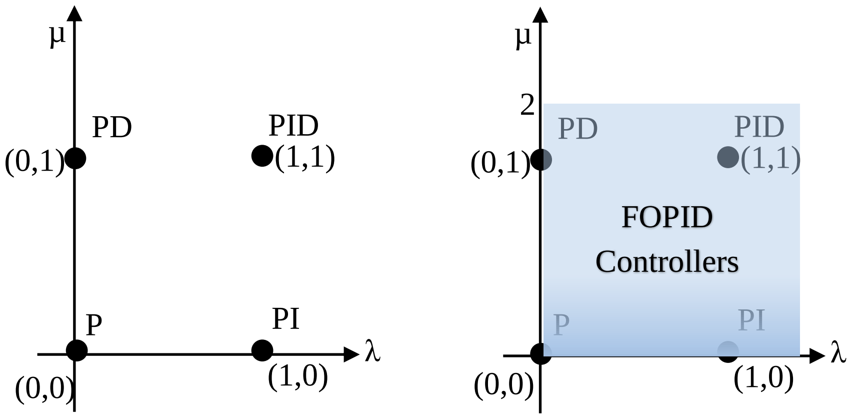

Figure 4.2 PID point and FOPID Plane [39]

As Figure 4.2 shown the FOPID controller expands the PID controller from point to plane. This expansion provides more flexibility for the controller design. This flexibility makes the system to against the change in setpoint and disturbance effect Therefore, the FOPID controller can control the process more accurately than the PID controller by providing robustness to the against noise, disturbance, and parameter variation[12].

The parameter variation of CSTR process is one of the main reasons for its nonlinearity behavior. FOPID controller has more capability against this uncertainty than PID controller due to its number of gain parameters and nonlinear behavior. Therefore, FOPID controller is selected as for the temperature control of CSTR process.

The mathematical equation of the FOPID controller is similar except for the integral and derivative order. The transfer function of the FOPID controller has the following form [40]:

Standard form:

$$\frac{U(s)}{E(s)} = K_p(1+\frac{1}{T_i s^{\lambda}}+T_d s^{\mu}) \tag{4.1a}$$

Parallel form:

$$\frac{U(s)}{E(s)} = K_p + \frac{K_i}{s^{\lambda}} + K_d s^{\mu} \tag{4.1b}$$

where $E(s)$ the error, and $U(s)$ the control input; K_p is the proportional gain, K_i is the integration gain, K_d is the derivative gain, T_i the integral time with $T_i = K_p / K_i$ and T_d the derivative time with $T_d = K_d/K_p$; λ and μ are the real number orders satisfying $0 < \lambda, \mu < 2$.

Figure 4.3 shows the structure of the FOPID controller.

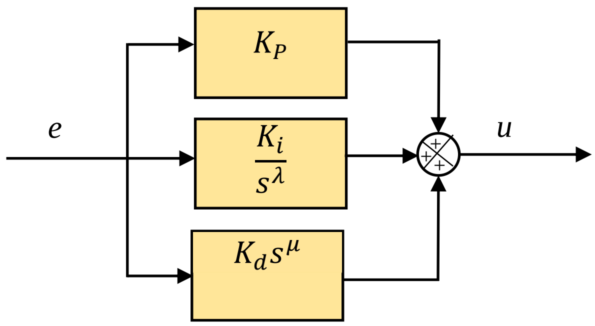

Figure 4.3 Structure of the FOPID controller [40]

Equation (4.1) can be represented in the time domain [41].

Standard form:

$$u(t) = K_p[e(t) + \frac{1}{T_i}\,{}_0D_t^{-\lambda} + T_d\,{}_0D_t^{\mu}] \tag{4.2a}$$

Parallel form:

$$u(t) = K_p e(t) + K_i\,{}_0D_t^{-\lambda} e(t) + K_d\,{}_0D_t^{\mu} e(t) \tag{4.2b}$$

The differ-integral operator, ${}_aD^{\alpha}_t$ in Equation (4.2), is defined by [40] [41]

$${}_aD_t^{\alpha} = \begin{cases} \frac{d^{\alpha}}{dt}, & \alpha > 0 \\ 1, & \alpha = 0 \\ \int_a^t (d\tau)^{-\alpha}, & \alpha < 0 \end{cases} \tag{4.3}$$

where $\alpha \in R$ is the order of the operator, and a and t are called lower and upper terminals, respectively.

There are several definitions for fractional derivatives, such as Grünwald-Letnikov (G-L) and Riemann-Liouville (R-L) definitions[42][43]. As one of the most commonly used definitions, G–L fractional differential/integral definition has the form [43]:

$$ {}_aD_t^{\alpha} f(t) = \lim_{h\to 0} h^{-\alpha} \sum_{j=0}^{n} \omega_j^{(\alpha)} f(t-jh), \qquad (4.4)$$

where h is the step size, $n = (t - a)/h$ the number of sampling points in a time interval $[a, t]$, and $\omega_j^{(\alpha)} = (-1)^j \begin{pmatrix}\alpha \\ j\end{pmatrix}$ is a polynomial coefficient of the sampling signal $f(t-jh)$, with $\begin{pmatrix}\alpha \\ j\end{pmatrix} = \frac{\alpha!}{j!(\alpha-j)!}$. Note that the fractional operator is a nonlocal operation over an interval $[a, t]$, i.e. the operator symbol ${}_aD^{\alpha}{}_t$ is explicitly expressed over the upper and lower terminals.

while the R-L definition is written as [43]

$$ {}_aD_t^{\alpha} f(t) = \begin{cases} \dfrac{1}{\Gamma(n-\alpha)} \dfrac{d^n}{dt^n} \displaystyle\int_a^t \dfrac{f(\tau)}{(t-\tau)^{\alpha-n+1}} d\tau, & n-1 < \alpha < n \\ \dfrac{1}{\Gamma(n-\alpha)} \displaystyle\int_a^t \dfrac{f(\tau)}{(t-\tau)^{\alpha+1}} d\tau, & \alpha < 0 \end{cases} \qquad (4.5)$$

where Γ is the Euler's gamma function. The Laplace transform of the R-L fractional derivative/integral (3) under zero initial conditions for the order α (0 < α < 1) is presented as [43]:

$$ L\left\{ {}_aD_t^{\pm\alpha} f(t) \right\} = s^{\pm\alpha} F(s) \qquad (4.6)$$

4.3 Genetic Algorithm as an Optimization Tool

Due to the nonlinear behavior of the process, the process operation is divided into two regions in this thesis work: low and high regions. FOPID controllers are designed for each region separately. In order to provide complete control for the process, the gain scheduling method is used. Each FOPID controller has 5 parameters, so a total of 10 parameters are tuned. Each FOPID controller is tuned using a GA for optimal performance.

A GA is a random search method that can be used to solve linear and nonlinear systems of equations and optimize complex problems especially in engineering applications [44]. GA uses probabilistic transition rules instead of deterministic rules and handles a population of potential solutions known as individuals or chromosomes that evolve iteratively. Each iteration of the algorithm is termed a generation. The evolution of solutions is simulated through a fitness function and genetic operators such as reproduction, crossover, and mutation [45]. The general structure the genetic learning algorithm is shown in Table 4.1.

Table 4.1 General structure of genetic learning algorithm [46].

Procedure GA(Gene)	Procedure Evaluation()
{	{
Initialization ();	For (k=0;k<Pop_size;k++
Evaluation ();	{
Keep_The_Best_Individual ();	Evaluate J fitness function;
Gen=0;	IF one of objective is not carried of THEN Repeat
Repeat{	{
Selection();	Reject the corresponding chromosome;
Crossover();	Regenerate another chromosome
Nonlinear mutation();	Calculation fitness Fit;
Evaluation();	}
Elitism strategies();	Until (All objectives satisfied)
Gen++;}	}
}	}

GA initially generates a random population, which is implemented with a smaller population size to allow the controller to optimize and converge at a faster rate. The initial population is established by encoding the FOPID parameters *Kp, Ki, Kd,* λ, and μ in strings called chromosomes. The fitness of each chromosome is calculated by the value that the FOPID parameter represents. Each set of FOPID parameters is passed to the FOPID controller [47].

The complete system response for each FOPID parameter value and its initial fitness value is calculated using a separate cost function. This process continues until the end of the generation that reaches the optimal fitness value. The ultimate goal of GA is to adjust the value of FOPID parameters (*Kp, Ki, Kd,* λ, μ) to the minimum value of the ability to operate the CSTR temperature control system within the entire range [47] [48]. The block diagram of GA implementation of temperature control of the CSTR process is shown in Figure 4.4.

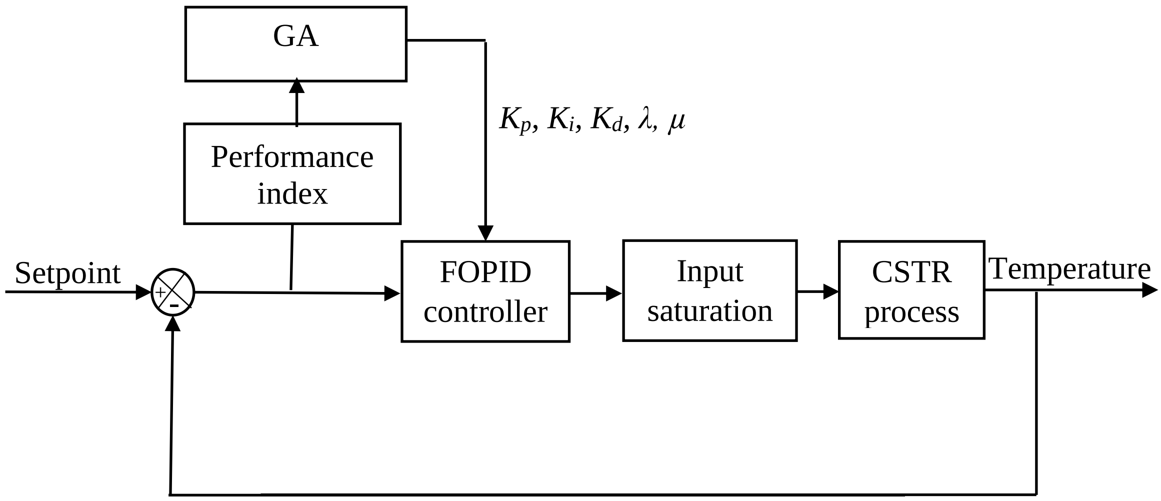

Figure 4.4 Block diagram of GA implementation in temperature control of CSTR

The overall response of the control system for each FOPID controller parameter value and initial values are used for parameter tuning. This process will be repeated until the end of generations that reach the optimal fitness value is achieved [49]. The control input is limited by saturation between -5 to 5.

$$\begin{cases} u_{\min} & \text{if } u < u_{\min} \\ u & \text{if } u_{\min} < u < u_{\max} \\ u_{\max} & \text{if } u > u_{\max} \end{cases} \tag{4.7}$$

where u_{min} =-5 and u_{max}=5

4.3.1 Performance Indices

The overall control system performance can be measured with different types of performance indices. This proved the quality of the controlled response by minimizing the integral of the error until the process has settled to its desired setpoint [50]. There are four common types of performance indices, Integral Absolute Error (IAE), Integral Square Error (ISE), Integral of Time Absolute Error (ITAE), and Integral of Time square Error (ITSE) [50].

Integral Absolute Error (IAE):

$$IAE = \int_0^\infty |e(t)|\, dt \tag{4.8}$$

Integral Square Error (ISE):

$$ISE = \int_0^\infty e^2(t)dt \tag{4.9}$$

Integral of Time Absolute Error (ITAE):

$$ITAE = \int_0^\infty t|e(t)|\, dt \tag{4.10}$$

Integral of Time Squared Error (ITSE):

$$ITSE = \int_0^\infty te^2(t)dt \tag{4.11}$$

IAE is used for the minimization of smaller errors than the larger ones. It also does not add weight to any of the errors in the process and this tends to produce a slower response than ISE but with less sustained oscillation. ISE is used for the minimization of large errors quickly, but it will tolerate small errors persisting for a long period. This leads to fast response but low amplitude and oscillation. The effect of ITAE and ITSE to weight the error which exists after a long time much more heavily than those at the start of the response. ITAE/ITSE produces the system with settling time much quicker than the above two methods (IAE and ISE) but also produces a system with sluggish initial response [51][52].

4.3.1.1 Integral Absolute Error and Control Signal

In this work, a performance index which is called Integral Absolute Error and Control Signal (IAEU) is used. IAEU is formed by the following equation [52].

$$IAEU = \int_0^\infty |e(t)| + w|\Delta u(t)|\, dt \tag{4.12}$$

where $e(t)$ is the error, that is, the difference between the setpoint and the output with y_s–y, w is the weighting factor and $\Delta u(t)$ is the deviation of control input with $\Delta u(t) = u(t) - u_0$. Given the value x_{10} of $x_1(t)$ and x_{20} of $x_2(t)$ in the steady-state, u_0 can be obtained from Equation (3.32) as

$$u_0 = \frac{(1+\beta)x_{20} + D_a H(1-x_{10})\exp(x_{20}/1+x_{20}/\gamma)}{\beta} \tag{4.13}$$

For $[x_{10}, x_{20}] = [0.0672,0]$

$$u_{01} = \frac{0.072\text{x}8(1-0.0672)\exp(0)}{0.3} = \text{-}1.7910$$

For $[x_{10}, x_{20}] = [0.4472,0.886]$

$$u_{02} = \frac{(1+0.3)\text{x}0.886+0.072\text{x}(1-0.1446)\exp(0.886/1+0.886/20)}{0.3} = 1.6605\text{e-}04$$

Then the control input signal in IAEU becomes

$$\Delta u_1 = u_1 - u_{01} = u_1 + 1.7910 \tag{4.14}$$

$$\Delta u_2 = u_2 - u_{02} = u_2 \text{-}1.6605\text{e-}04 \tag{4.15}$$

IAEU is used not only to achieve satisfactory dynamic characteristics in the transition process but also to prevent the control input from becoming excessively large. In particular, it has the advantage of being able to adjust the size according to the relative importance of the error and the control input by adjusting the weighting factor. Therefore, IAEU is a more suitable performance index for the temperature control of CSTR than others methods.

4.4 Fuzzy Gain Scheduling

4.4.1 Gain Scheduling

Most industrial processes used PID controllers due to ease of implementation and having less cost. However, this controller gives satisfactory performance only on a specified operating region of the system. Since the amount of product via the CSTR process depends on the demand of customers, this leads to having variable temperature operating points and instability in the system. As a result, the FOPID controller having more degrees of freedom is used for this research work. For the CSTR system, two FOPID controllers are applied by considering only two operating points and should be properly switched based on the operating points range. The switching can be done manually using toggle switches but this is a very tedious task and can’t be robust due to ON and OFF control mechanisms. An automatic switching system is required to mitigate these problems.

Gain scheduling is a common approach to control nonlinear processes. It involves the application of different controller tunning parameters as a process transitions from one operating range to another [53]. In this way, controller parameters can be more closely aligned with the process’s nonlinear dynamics. to identify the current operating region on the system, scheduling variables are used. [54] [55].

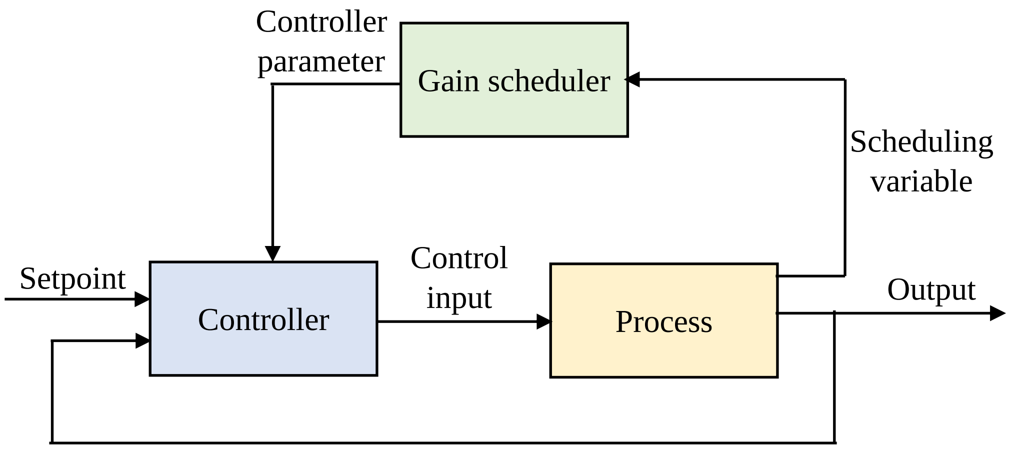

Figure 4.5 General block diagram of gain scheduling method [55].

Figure 4.5 shows the block diagram of a typical gain scheduling system. There may be two or more controllers in the block diagram. The controller parameters are tuned by a tuning mechanism according to the operating region. Then gain scheduler is selected the proper controller according to the scheduler variable value.

4.4.2 Design of a Fuzzy Gain Scheduler

In designing a gain scheduled control system, several controllers are in general designed and joined together by a switching decision or smooth interpolation. Abrupt change of controller parameters introduces unexpected results. Due to this reason, fuzzy logic is frequently used to realize the scheduling scheme for switching the controller parameters because it allows smoothly varying nonlinear functions. It has an advantage if the operating range is large. Figure 4.6 shows the structure of a fuzzy modeling system.

A fuzzy system design has different steps [56]. Determining the input and output variables of the system is the first step. In the second step, the universe of information is divided into the number of fuzzy subsets and the linguistic label is assigned for each subset. Getting membership function for each subset is the third step. The third step is to obtain the membership function of each fuzzy subset. The fuzzification process starts from the fourth step. The fifth step is the configuration of the fuzzy rule base. The fuzzy rule base is formulated by assigning the relationship between fuzzy input and output. In the sixth step, the fuzzy outputs are combined by applying the fuzzy inference to locate the fuzzy outputs and merge them. Finally, the defuzzification process is starting to convert the fuzzy outputs into crisp outputs.

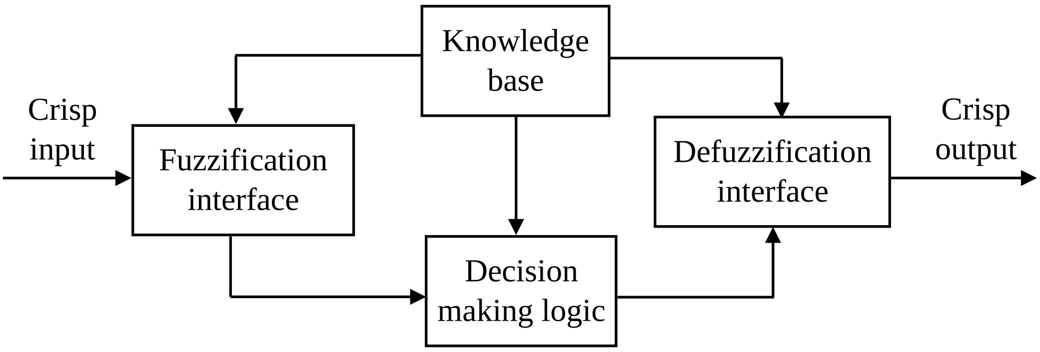

Figure 4.6 The general structure of fuzzy modeling system [56]

The sixth step is combining fuzzy outputs, by applying fuzzy reasoning to locate fuzzy outputs and merge them. Finally, initiate the defuzzification rule to form a crisp output. In the most general form, the knowledge of a fuzzy system can be represented by fuzzy models consisting of if-then rules. The fuzzy model is classified as Mamdani-type and Sugeno--type. The Sugeno-type fuzzy model has the advantage of using the no defuzzification process.

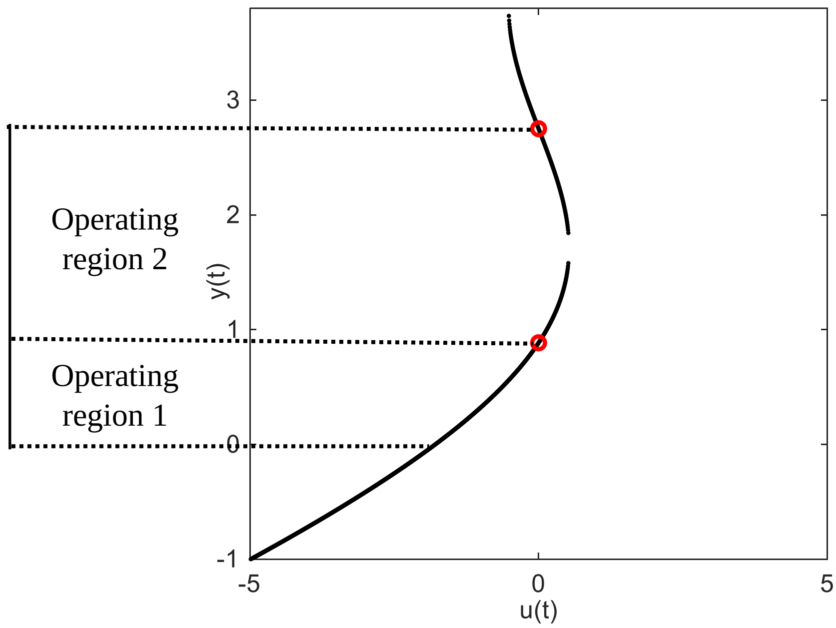

Figure 4.7 Operating regions of the CSTR process

In this study, the CSTR is considered to operate in the dimensionless temperature range of 0 and 2.750 as depicted in Figure 4.7. As examined in Figure 3.6, shows a large nonlinearity according to temperature, so the temperature is considered to be the scheduling variable. The scheduling variable range is partitioned by two fuzzy sets. The two FOPID controllers as local controllers are combined by a fuzzy model.

4.4.2.1 Takagi-Sugeno Fuzzy modeling

Takagi Sugeno (TS) type fuzzy model was proposed by Takagi and Sugeno in 1985. It is expressed in the form of IF-THEN, in which the consequent part does not form a fuzzy set, but is expressed in the form of a constant or in the linear equation input variable. The typical fuzzy rules in the TS have the following form [57]:

$$\text{If } x_1 \text{ is } A \text{ and } x_2 \text{ is } B \text{ then } z=f(x_1, x_2) \tag{4.16}$$

where A and B are fuzzy set in the antecedent and $z= f(x_1, x_2)$ is a crisp function in the consequent. For example, if there are two inputs and three rules:

$$\text{Rule 1: if } x_1 \text{ is } A_1 \text{ and } x_2 \text{ is } B_1\text{, then } z_1=f_1(x_1, x_2) \tag{4.17a}$$

$$\text{Rule 2: if } x_1 \text{ is } A_2 \text{ and } x_2 \text{ is } B_2\text{, then } z_2=f_2(x_1, x_2) \tag{4.17b}$$

$$\text{Rule 3: if } x_1 \text{ is } A_3 \text{ and } x_2 \text{ is } B_3\text{, then } z_3=f_3(x_1, x_2) \tag{4.17c}$$

Then, the inferred output is the weighted average of all rules output and calculated as

$$\begin{aligned} z &= \frac{\alpha_1 z_1 + \alpha_2 z_2 + \alpha_3 z_3}{\alpha_1 + \alpha_2 + \alpha_3} \\ &= \frac{\alpha_1 f_1(x_1, x_2) + \alpha_2 f_2(x_1, x_2) + \alpha_3 f_3(x_1, x_2)}{\alpha_1 + \alpha_2 + \alpha_3} \end{aligned} \tag{4.18}$$

where α_i denotes the i^{th} truth value with $\alpha_i = T[A_i(x_1), B_i(x_2)]\ (i = 1, 2, 3)$, $A_i(x_1)$ and $B_i(x_2)$ the membership grades, and T fuzzy combination referred to as "T-norm". The minimum or multiplication operator can be used the corresponding truth value.

Therefore, in general, for the rules of N, the final output result can be calculated as [58]

$$z = \frac{\sum_{i=1}^{N} \alpha_i z_i}{\sum_{i=1}^{N} \alpha_i} \tag{4.19}$$

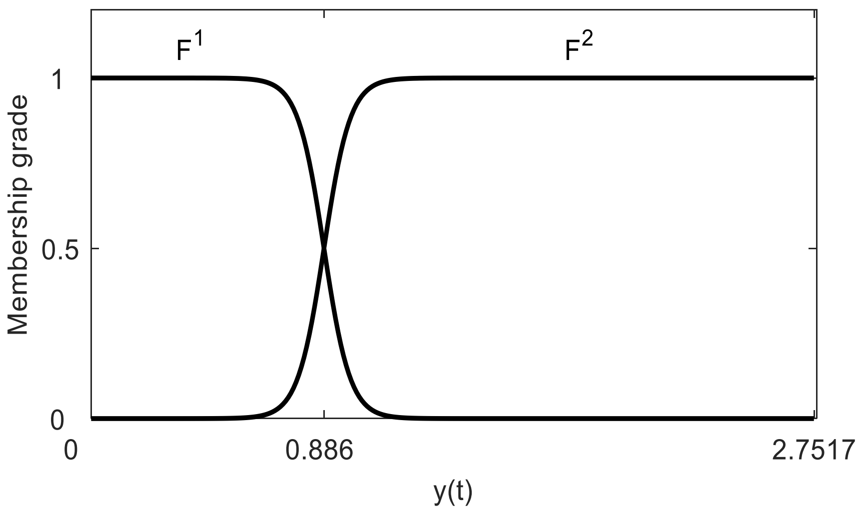

Figure 4.8 Membership functions defined over *y(t)*

In this thesis work, two fuzzy sets are defined over the temperature variable x_2 (= y) of the CSTR process. Their membership functions are shown in Figure 4.8.

Each membership function of the fuzzy set is defined by the sigmoid function:

$$F_i(y; a_i, c_i) = \frac{1}{1+e^{a_i(y-c_i)}} \quad (i = 1,2) \tag{4.20}$$

where two parameter values are set to $[a_1, c_1]$ = [-20, 0.886] for F_1 and $[a_2, c_2]$ = [20, 0.886] for F_2. The value of 0.886 is the reflection point as well as one equilibrium point and if the value of 20 is negative, the left side is opened, and if it is positive the right side is opened.

Since the output (temperature) or the input to the controller are real numbers (not linguistic words), it is assumed to be a fuzzy singleton. Based on the definition of fuzzy theory, a T-S fuzzy model is selected as the fuzzy gain scheduler:

$$\text{Rule1: if } y(t) \text{ is } F_1, \text{ then } u_1(t) = K_{p1}e(t) + K_{i1}\,{}_0D_t^{-\lambda_1}e(t) + K_{d1}\,{}_0D_t^{\mu_1}e(t) \tag{4.21a}$$

$$\text{Rule2: if } y(t) \text{ is } F_2, \text{ then } u_2(t) = K_{p2}e(t) + K_{i2}\,{}_0D_t^{-\lambda_2}e(t) + K_{d2}\,{}_0D_t^{\mu_2}e(t) \tag{4.21b}$$

where $y(t)$ and $u_i(t)$ (i=1,2) mean the input and output variables of the fuzzy system, respectively; F_i (i=1,2) fuzzy sets of the fuzzy system; K_{pi}, K_{ii}, K_{di}, λ_i and μ_i (i=1,2) are the parameters of the FOPID controller.

Then, the inferred result is expressed by:

$$
\begin{aligned}
u(t) &= \frac{a_1 u_1(t) + a_2 u_2(t)}{a_1 + a_2} \\
&= h_1[K_{p1}e(t) + K_{i1\,0}D_t^{-l_1}e(t) + K_{d1\,0}D_t^{m_1}e(t)] \\
&\quad + h_2[K_{p2}e(t) + K_{i2\,0}D_t^{-l_2}e(t) + K_{d2\,0}D_t^{m_2}e(t)]
\end{aligned} \tag{4.22}
$$

where α_i (i=1,2) is the truth value of each control rule and $\eta_i = \alpha_i/(\alpha_1+\alpha_2)$.

Based on Equation (4.22) the fuzzy system combined the two controllers and give one control output to the CSTR process.

CHAPTER FIVE

RESULT AND ANALYSIS

In this chapter, the simulation results and analysis of the proposed fuzzy gain scheduling of the FOPID control system for the CSTR process are discussed. In addition for the comparison purpose, the PID controller tuned by the CHR method [21] and the adaptive nonlinear bounded controller[22] is implemented. The response analysis is done based on the setpoint tracking and disturbance rejection capabilities. The parameter setting for each controller (proposed, adaptive, and PID CHR) are described in the following sections. The performance comparison is done based on their rise time, settling time, overshoot, and IAE.

5.1 Parameter Settings of the CSTR Process

The dimensionless mathematical modeling of the CSTR process has been used the nominal parameters including the Damköhler number (D_a), the heat of reaction(H), the heat transfer coefficient (β), and the ratio of activation energy to kinetic energy (γ). Since the modeling equation of the CSTR process is dimensionless, the nominal parameter values have no units. Table 5.1 shows the nominal parameter values used for simulation.

Table 5.1 Nominal parameter values of the CSTR process [35]

Parameter name	Nominal value
D_a	0.072
H	8
β	0.3
γ	20

5.2 Controller Parameter Settings

5.2.1 Parameter Settings of the FOPID controller

As can be seen in Chapter 4, the two local FOPID (FOPID1 and FOPID2) controllers are used for the low (stable region) and high (unstable region) separately based on the operating ranges. From 0 to 0.886 is the lower region and from 0.886 to 2.7517 is the upper region. FOPID1 controller has five tuning parameters K_{p1}, K_{i1}, K_{d1}, λ_1, and μ_1 and FOPID2 controller also has five parameters, K_{p2}, K_{i2}, K_{d2}, λ_2, and μ_2. Based on the process parameter values in

Table 5.1, the parameters of the FOPID controller at each operating point were optimally tuned using a GA. The details of GA parameter settings used in the simulation for setpoint tracking and disturbance rejection are shown in Table 5.2.

Table 5.2 GA parameter settings for optimization

Parameter	Setpoint tracking	Disturbance rejection
	Value	Value
Maximum generation	30	30
Population size	30	30
Number of parameters	5	5
Lower boundary	[0 0 0 0 0]	[0 0 0 0 0]
Upper boundary	[30 30 30 2 2]	[300 300 30 2 2]

For optimal setpoint tracking response, the FOPID1 controller parameters were tuned for minimization of the objective function in Equation (4.10) while y_s was changed from 0 to 0.886. The graphical result of GA optimization with their best and mean fitness values are shown in Figure 5.1 and its minimum best fitness value is 2.52835.

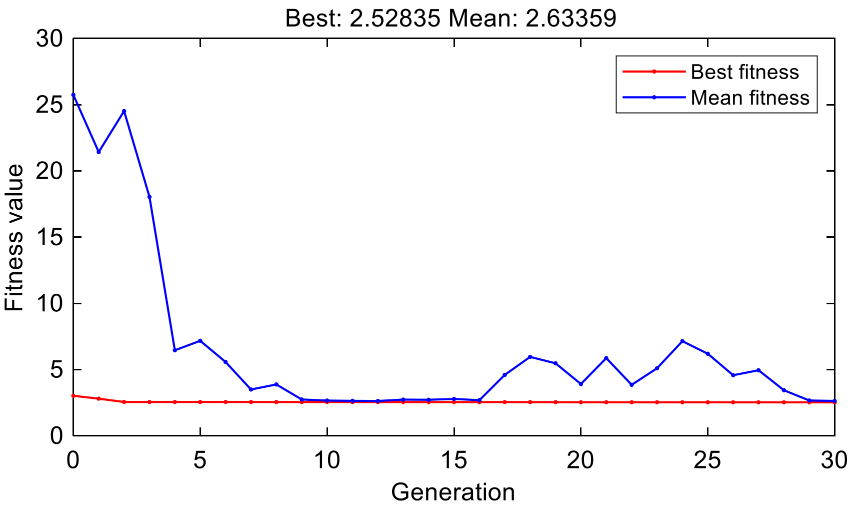

Figure 5.1 Fitness value vs generation for operating 1 region

The tuning of the FOPID2 controller parameter for the second operating point was also performed based on GA optimization. The parameters were tuned when y_s is changed from 0.886 to 2.7517. The graphical result is shown in Figure 5.2 and the best-optimized value is 4.08593.

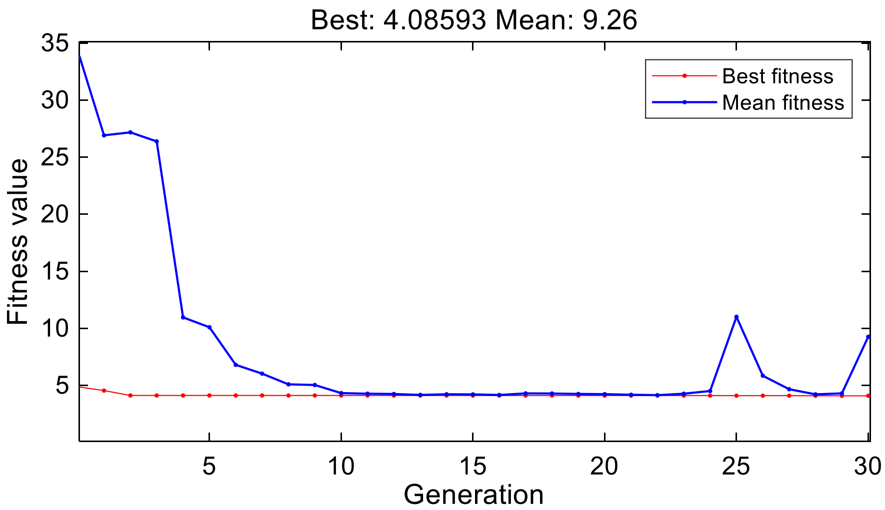

Figure 5.2 Fitness value vs generation for operating 2 region

For optimal disturbance rejection response, the FOPID1 controller parameters were tuned for minimization of the objective function in Equation (4.10) while y_s was kept to 0.886, d_1 and d_2 were changed from 0 to 0.5 and -0.5, respectively.

Table 5.3 FOPID controller parameters for setpoint tracking and disturbance rejection

Local controller	Parameter	Setpoint tracking	Disturbance rejection
		Value	Value
FOPID1	K_{p1}	0.3226	242.648
	Ki_1	12.7873	285.067
	K_{d1}	2.5438	1.636
	λ_1	0.0238	1.057
	μ_1	0.4174	0.780
FOPID2	K_{p2}	0.3851	242.222
	K_{i2}	10.9436	287.067
	K_{d2}	2.4501	1.386
	λ_2	0.0238	1.077
	μ_2	0.4019	0.520

The FOPID2 controller parameters were also tuned while y_s was kept to 0.886, d_1, and d_2 were changed from 0 to -0.5 and 0.5, respectively. The optimized parameter values of the two local FOPID controllers are shown in Table 5.3.

5.3 Results of FOPID 1 and FOPID 2 controllers

As discussed in the modeling section the system is simulated in two operating regions. Using the FOPID1 controller, the result of the proposed system response is shown in Figure 5.3. The system is simulated based on the low region of 0.886 setpoints.

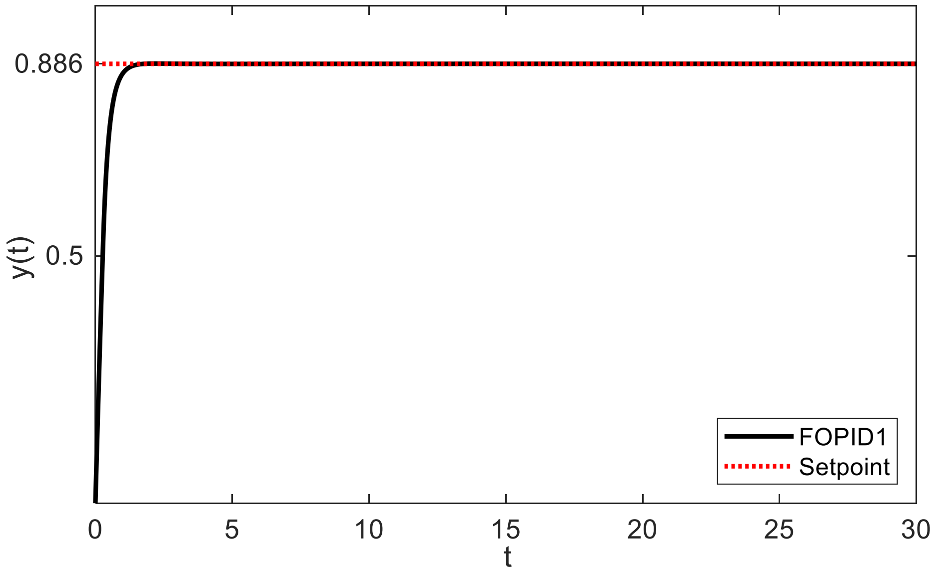

Figure 5.3 The result of the FOPID1 controller using GA

When the setpoint is increased from 0 to 0.886, the response of the controlled variable is tracking the setpoint with 0% overshoot and 1.0232 settling time. This shows the effectiveness of the FOPID1 controller for the dimensionless temperature control of CSTR process in region one.

The second FOPID2 controller is performed based on the setpoint range of 0.886 to 2.7517 in the second operating range as shown in Figure 5.4. The graphical result shows the system has a 4.8159% overshoot with a 2.4596 settling time.

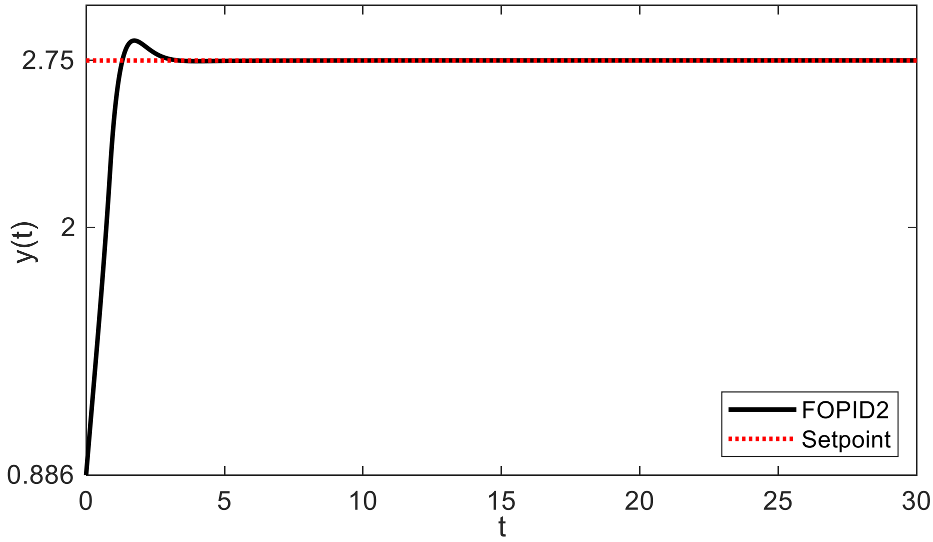

Figure 5.4 The result of FOPID2 controller using GA

5.4 Implementations of existing controllers

5.4.1 Parameter Settings of the PID Controller

The PID controller parameters were tuned using the CHR method as mentioned in Section 2.3.1 for comparison purposes. Since this method is based on the three parameters (K, T, L) of the first-order time delay (FOPTD) model of the CSTR process, a GA was used to identify the FOPTD parameters in Equation (2.3) by employing the model adjustment scheme. The GA adjusts the parameters of the FOPTD model so that the same input is imposed on the model connected in parallel with the CSTR process, and the model output $y_m(t)$ is compared with the CSTR output $y(t)$ so that the error becomes small. For this, the following IAE criterion was used to find out the optimal parameters.

$$IAE = \int_0^\infty |\, y(t) - y_m(t) \,|\, dt \qquad (5.1)$$

Parameter settings of the GA optimization for calculation of the PID controller parameters K, T, and L is shown in Table 5.4.

Table 5.4 Parameter settings of GA optimization for PID controller

Parameter	Value
Maximum generation	50
Population size	20
Number of parameters	3
Lower boundary	[0 0 0]
Upper boundary	[5 5 1]

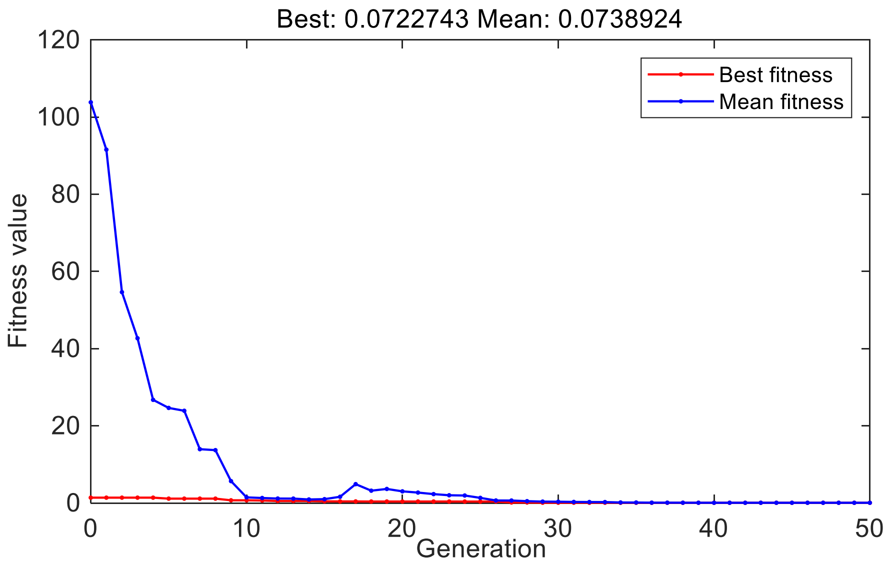

Figure 5.5 GA optimization with a minimum object function

The fitness function graphical result of GA optimization is shown in Figure 5.5 and the values of the estimated parameters are listed in Table 5.5.

Table 5.5 Estimated parameters of the FOPTD model

Parameter	Value
K	0.495
T	1.838
L	0.049

As a result, depending on Equation (2.3) the FOPTD process transfer function with time delay is calculated as

$$G(s) = \frac{0.4946}{1+1.8376s} e^{-0.0494s} \tag{5.2}$$

A simulation has been carried out by applying the same parameter for the PID controller to check the similarity of the two systems. As can be seen from the graphical result shown in Figure 5.6, the FOPTD and CSTR process has the same result. Therefore, for the comparison purpose, the above parameters are used for the simulation of the CSTR process using PID controller.

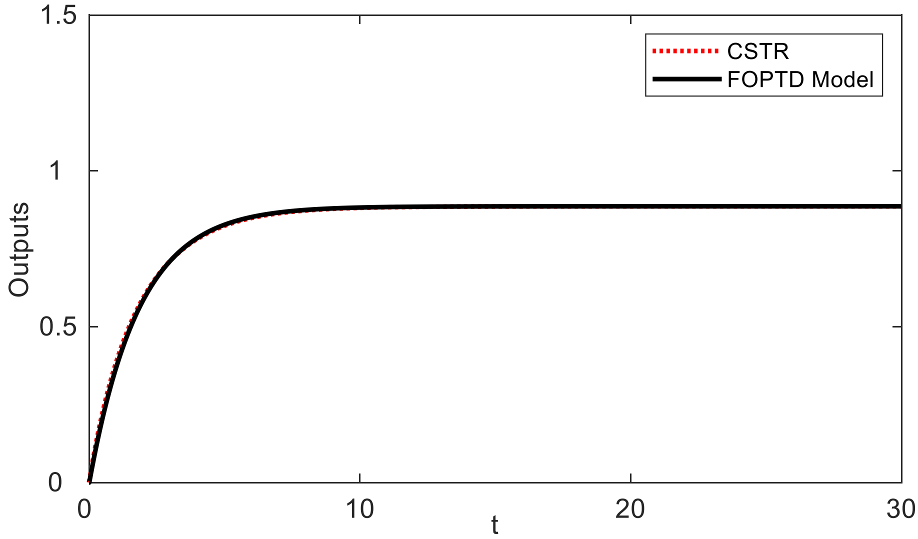

Figure 5.6 FOPTD vs CSTR process

Based on Equation (5.2), the PID controller gains are calculated by the CHR method and listed in Table 5.6 for both setpoint tracking and disturbance rejection.

Table 5.6 CHR settings of the PID controller for setpoint tracking and disturbance rejection

Parameters	Setpoint tracking	Disturbance rejection
	With 0% overshoot	With 0% overshoot
K_p	45.125	71.448
K_i	24.556	605.4915
K_d	1.114	1.484

5.4.2. Parameter Settings of Adaptive Nonlinear Control

The bounded nonlinear controller that has been enabled to learn the controller process adaptively have some parameter includes slope (gain factor), bias(threshold) and learning rating. The parameters used for temperature control of the CSTR process are listed in Table 5.7 [22].

Table 5.7 parameter value for the adaptive learning algorithm

Parameter	Value
B	5
θ	0.2
η	> 0
$sign\left(\frac{\partial y}{\partial t}\right)$	1

5.5 Discussions of Setpoint Tracking Responses

A setpoint tracking performance of temperature control of CSTR is measured based on the swiftness and closeness of the response. Swiftness is a capability for the output to quickly follow the setpoint and assessing by rising time(t_r). Closeness is the properties for the output to match the setpoint and assessing by overshoot (M_p), settling time(t_s), and IAE. In this section, the comparison analysis is done among the proposed method, the PID-CHR controller, [21] and the adaptive controller [22]. Hereafter, the proposed method is denoted as FOPID-Proposed, the PID controller tuned by the CHR method as PID-CHR, and the adaptive controller proposed by Chen and Peng as Adaptive Control-CP.

compare the setpoint tracking performance, four scenarios were considered.

- Scenario 1 (UP-UP setpoint changes): the setpoint tracking response according to this scenario is implemented when the setpoint is increased from 0 to 0.886 (first UP) then after a time of 15 again it is increased from 0.886 to 2.751 (then UP).
- Scenario 2 (UP-DOWN setpoint changes): the setpoint tracking response according to this scenario is performed, by assuming that when the setpoint is increased step wisely from 0 to 0.886 then at the time of 15 it is decreased from 0.886 to 0.
- Scenario 3 (DOWN - UP setpoint changes): In Scenario 3, the tracking response is simulated when the setpoint is decreased step wisely from 2.751 to 0.886 then at the time of 15 it is increased from 0.886 to 2.751.

- Scenario 4 (DOWN - DOWN setpoint changes): In Scenario 4, the tracking response is simulated when the setpoint is decreased step wisely from 2.751 to 0.886 then at the time of 15 it is decreased from 0.886 to 0.

5.5.1 Response to Scenario 1

Based on this scenario, the setpoint tracking responses of the proposed, PID-CHR, and Adaptive control-CP methods are shown in Figure 5.7. When the setpoint increases step wisely from 0 to 0.886, the output *y(t)* is increased and tracks the desired response. As a result, the process is reached at a stable equilibrium point $\boldsymbol{x}_a$= [0.1446, 0.8860]^T. Then at *t*=15, the setpoint is increased from 0.886 to 2.751, and *y(t)* is also increasing closely to 2.7517 and then, the process is reached at unstable equilibrium point $\boldsymbol{x}_b$= [0.4472 2.7517]^T.

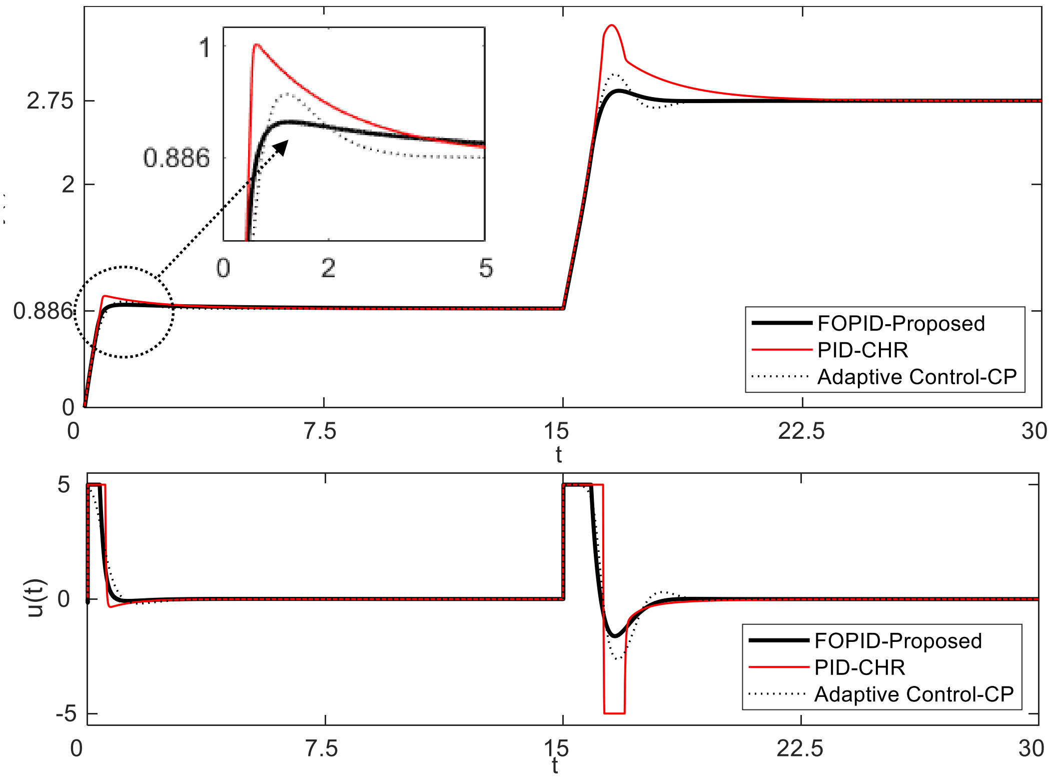

Figure 5.7 UP-UP setpoint tracking Comparison response

Figure 5.2 also explains the output of the controller signal *u(t)*, which shows the accumulation of error multiplied with gains and it should be between the saturation value of (-5, 5). As it can be seen in the graphical result, when y_s is increased from 0 to 0.886, the proposed method has 4.028% overshoot, whereas PID-CHR and adaptive controllers have overshoot 13.02% and 7.32% respectively. Also, the settling time of the proposed method is 4.0373. In addition, the IAEU value of the proposed method is 0.2671.

When y_s is increased from 0.886 to 2.7517, the proposed method has an overshoot of 4.819%, a settling time of 2.4289, and 1.2150 of *IAE*. The general performance parameter results of the three methods during the UP-UP setpoint tracking are shown in Table 5.8. In general, the proposed method provides has better performance in all aspects.

Table 5.8 Setpoint tracking performance for UP-UP response

Methods	$y_s = 0 \rightarrow 0.886$			
	t_r	M_p	t_s	*IAE*
FOPID-Proposed	0.4266	0.04028	4.0373	0.2671
PID-CHR	0.4538	0.1302	4.0483	0.4359
Adaptive control-CP	0.6266	0.0732	4.3806	0.3305
	$y_s = 0.886 \rightarrow 2.7517$			
FOPID-Proposed	0.9466	0.04819	2.4289	1.2150
PID-CHR	0.9794	0.3638	6.0839	2.2063
Adaptive control-CP	1.0563	0.12734	3.3913	1.3700

5.5.2 Response to Scenario 2

the UP-DOWN setpoint tracking response of dimensionless temperature control of a CSTR process is shown in Figure 5.8. Based on the graphical result, the comparative performance parameters for the FOPID-Proposed, PID-CHR, and Adaptive control-CP methods are shown in Table 5.9. For the first region, when the setpoint increased from 0 to 0.886, the proposed method has a 4.028 % overshoot which is better than the other two methods. Also, the settling time of the proposed FOPID method has 4.0373 and its performance index function IAE value is 0.2671.

From the second region, when the setpoint changes from 0.886 to 0 setpoint, the overshoot in case of the proposed method is 2.3668, which is smaller than the PID-CHR method but a little higher than Adaptive control method. The settiling time of the controlled variable in case of the proposed method is 1.6757 and IAE is 0.4046.

For the UP-DOWN simulation comparison analysis, the proposed method shows better performance in case of settling time, overshoot, and IAE results as compared to the other two techniques.

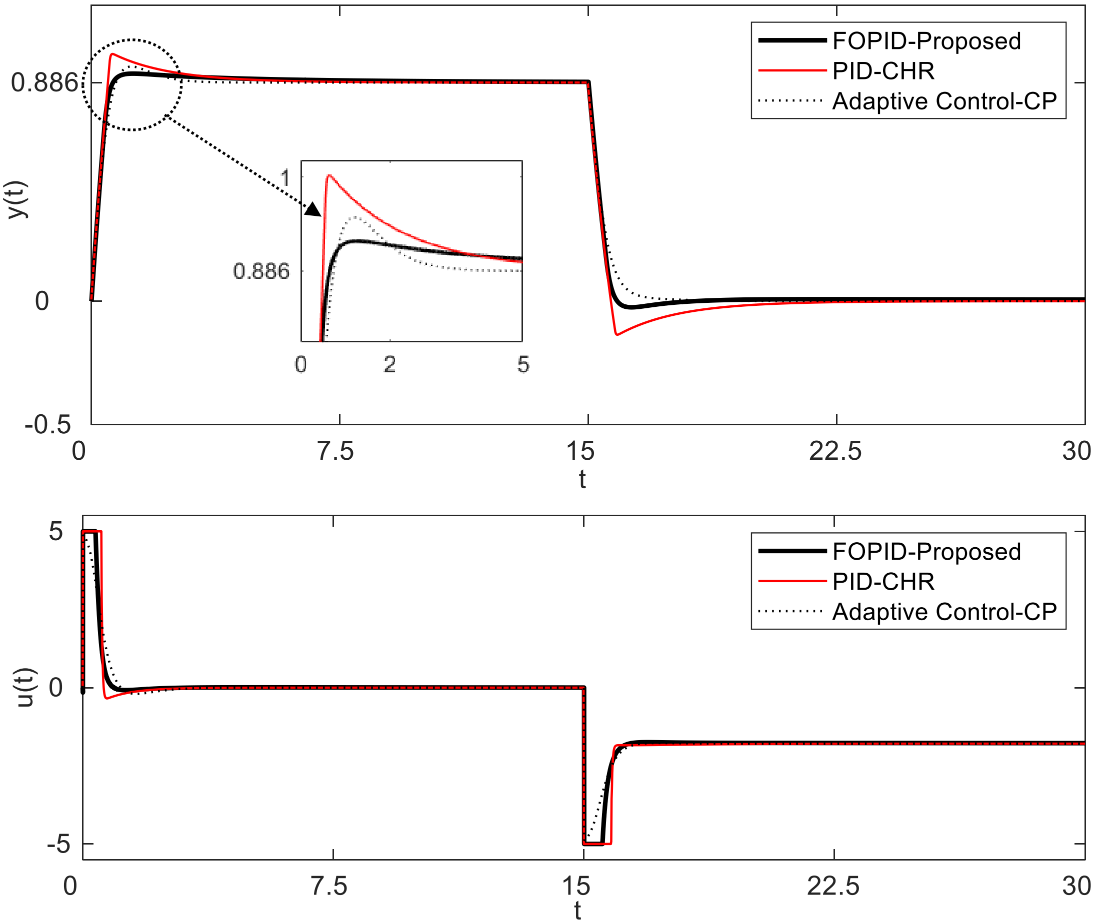

Figure 5.8 UP-DOWN setpoint tracking comparison response

Table 5.9 Setpoint tracking performance for UP-DOWN

Methods	$y_s = 0 \rightarrow 0.886$			
	t_r	M_p	t_s	IAE
FOPID-Proposed	0.4266	0.04028	4.0373	0.2671
PID-CHR	0.4538	0.1302	4.0483	0.4359
Adaptive control-CP	0.6266	0.0732	4.3806	0.3305
$y_s = 0.886 \rightarrow 0$				
FOPID-Proposed	0.561	0.023668	**1.6757**	**0.4046**
PID-CHR	0.6155	0.15101	4.6932	0.5492
Adaptive control-CP	1.180	0.0000	2.4412	0.4057

5.5.3 Response to Scenario 3

The graphical setpoint tracking response using the three control methods for the dimensionless analysis of a CSTR process is shown in Figure 5.9.

For the first region, when the setpoint decreased from 2.751 to 0.886, the proposed method has no overshoot whereas the PID -CHR and Adaptive controllers have 25.072% and 4.442% overshoot respectively. So, the proposed method is better than the other two methods in the case of overshoot reduction analysis. Also, the settling time of the proposed FOPID method has 1.3801 which is better than the PID-CHR and adaptive methods.

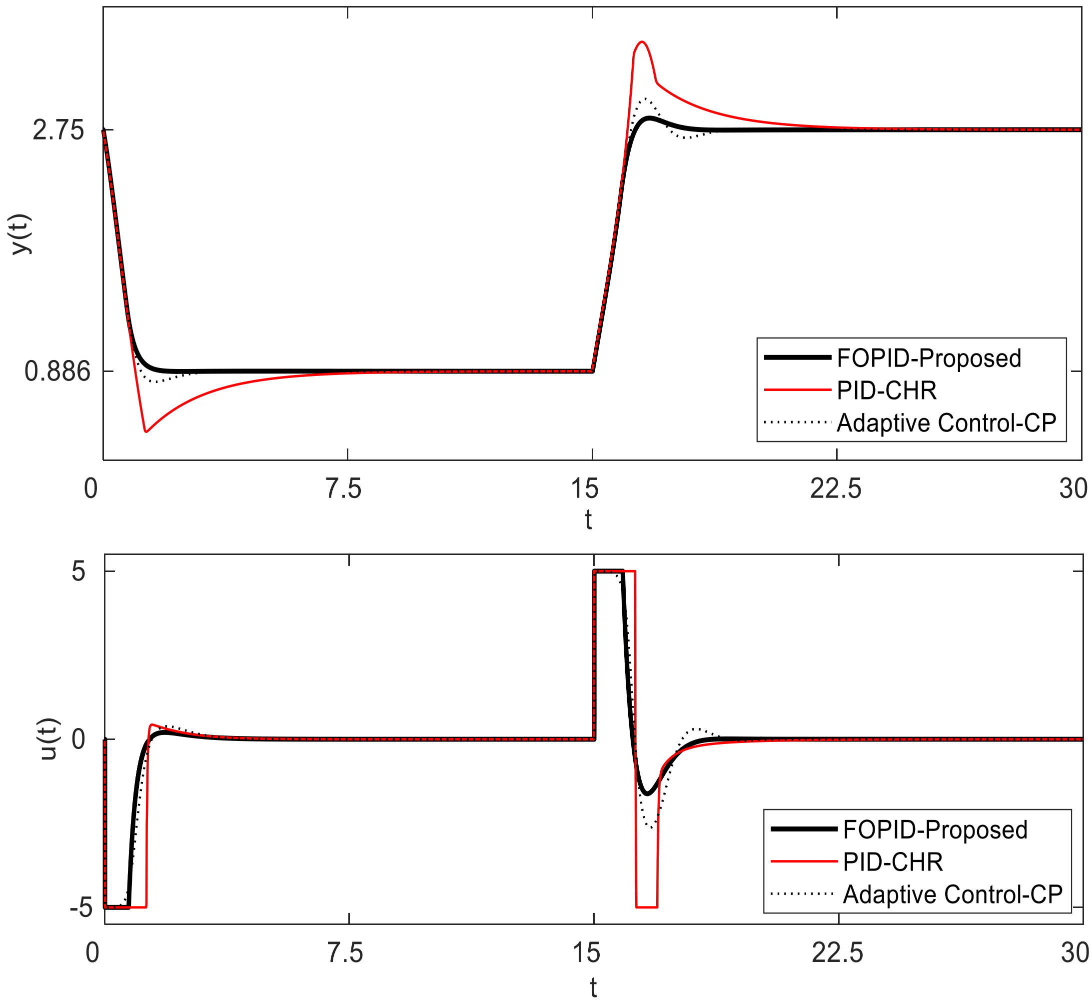

Figure 5.9 DOWN-UP setpoint tracking comparsion response

From the second region, when the setpoint increases from 0.886 to 2.751, the overshoot in the case of the proposed method is 4.819, which is smaller than the other two methods. The settling time of the controlled variable in the case of the proposed method is 2.4289. The details of the comparative performance parameters result for the proposed FOPID, PID -CHR, and Adaptive control methods are shown in Table 5.10. Therefore, in all cases of the comparative parameter results, the proposed method has better performance than others.

Table 5.10 Setpoint tracking performance for DOWN-UP response

Methods	y_s =2.7517 $\rightarrow$ 0.886			
	t_r	M_p	t_s	*IAE*
FOPID-Proposed	1.0865	0.000	1.3801	1.2997
PID-CHR	0.7820	0.2507	5.9662	2.064
Adaptive control-CP	0.8246	0.0442	2.3617	1.3700
y_s =0.886 $\rightarrow$ 2.7517				
FOPID-Proposed	0.9466	0.04819	2.4289	1.2150
PID-CHR	0.9794	0.3638	6.0839	2.2063
Adaptive control-CP	1.0563	0.12373	3.3913	1.3700

5.5.4 Response to Scenario 4

DOWN-DOWN setpoint tracking response of dimensionless temperature control of CSTR process is shown in Figure 5.10. when y_s decreases from 2.7517 to 0.886, the proposed method overshoot is 0% and has a settling time of 1.380. When y_s decreases from 0.886 to 0, the proposed method has no overshoot (0%), and PID -CHR and Adaptive controller has 15.35 % and 4.167% respectively. Also, the proposed method has a settling time of 1.6757 which is better than the other two methods.

Based on the result of the DOWN-DOWN setpoint tracking response, the performance parameter result is shown in Table 5.11. As a result, in all cases, the proposed method has better performance than others.

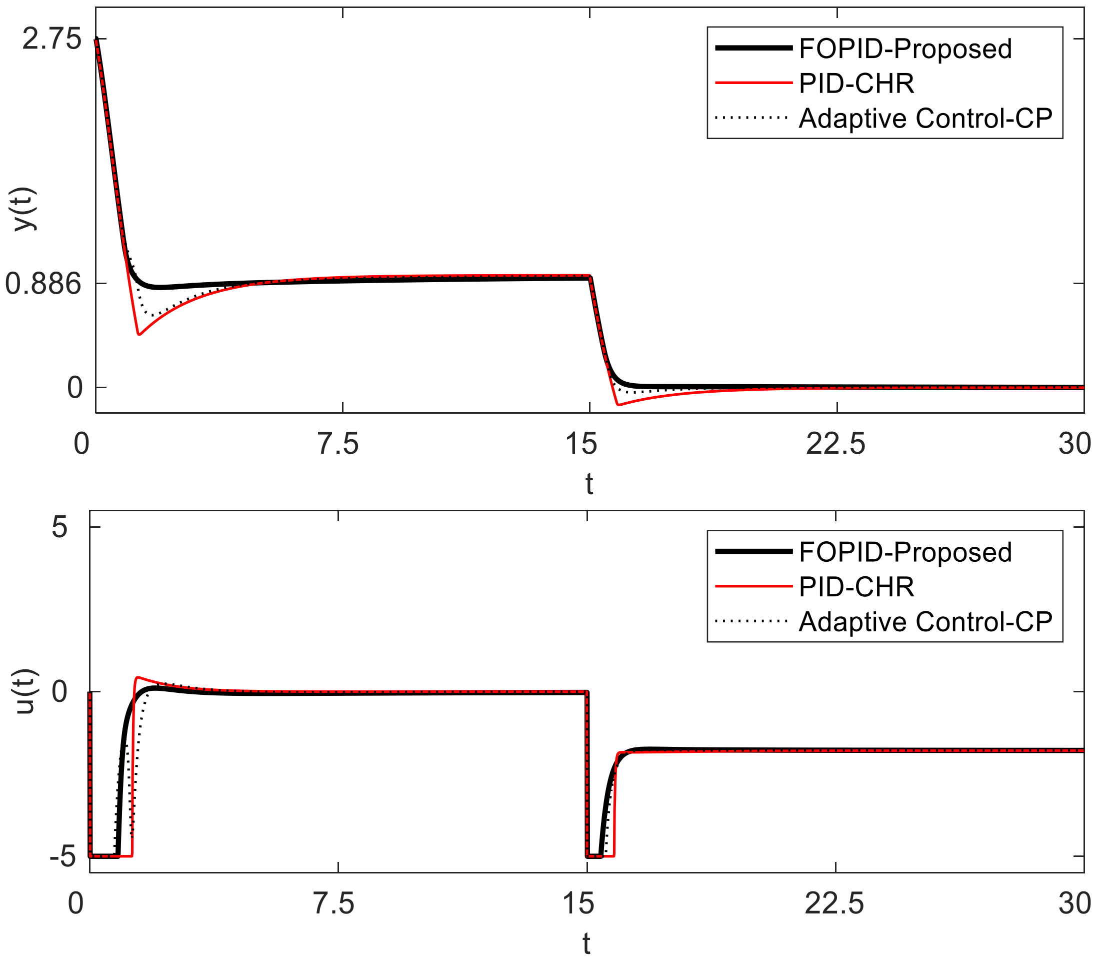

Figure 5.10 DOWN-DOWN setpoint tracking comparison response

Table 5.11 Setpoint tracking performance for DOWN-DOWN response

Methods	y_s =2.7517 ⟶ 0.886			
	t_r	M_p	t_s	IAE
FOPID-Proposed	1.0865	0.000	1.3801	1.2997
PID-CHR	0.7820	0.2507	5.9662	2.064
Adaptive control-CP	0.8246	0.0442	2.3617	1.3700
y_s = 0.886 ⟶ 0				
FOPID-Proposed	1.1806	0.000	1.6757	0.4046
PID-CHR	0.6153	15.350	4.6932	0.5492
Adaptive control-CP	0.666	4.1672	2.4412	0.4057

5.6 Simulation of Disturbance Rejection Responses

In the CSTR process two disturbance is assumed, on the inlet concentration d_1 and inlet temperature d_2. To demonstrate the disturbance rejection performance of the proposed method, a set of simulation works based on two scenarios were conducted.

- Scenario 1: while the setpoint y_s was kept at 0.866 (stable equilibrium), disturbance d_1 was increased and d_2 was decreased.
- Scenario 2: while the setpoint y_s was kept at 0.866 (stable equilibrium), disturbance d_1 was decreased and d_2 was increased.

5.6.1 Response to Scenario 1

The response of the three methods is performed when disturbance d_1 changes from 0 to 0.5 and d_2 changes from 0 to -0.5 step wisely at a time of 0. For understanding purposes, the setpoint is kept constant at 0.886. A graphical result is plotted for the proposed method, PID-CHR, and adaptive controllers as shown in Figure 5.11. Therefore, the proposed plant initially stays away from the equilibrium point due to disturbances and after a moment the effect of disturbance is eliminated and it returns to the steady-state due to the control action.

For the comparison of controllers in case of disturbance rejection response, the performance parameters of pick time, recovery time, overshoot, and *IAE* are considered. Based on the simulation result, the proposed FOPID controller has a recovery time and overshoot of 7.3426 and 0.71% respectively. The additional parameters are listed in Table 5.12. As can be seen from the graphical and tabular results, the proposed method has better performance parameter results when disturbance is considered.

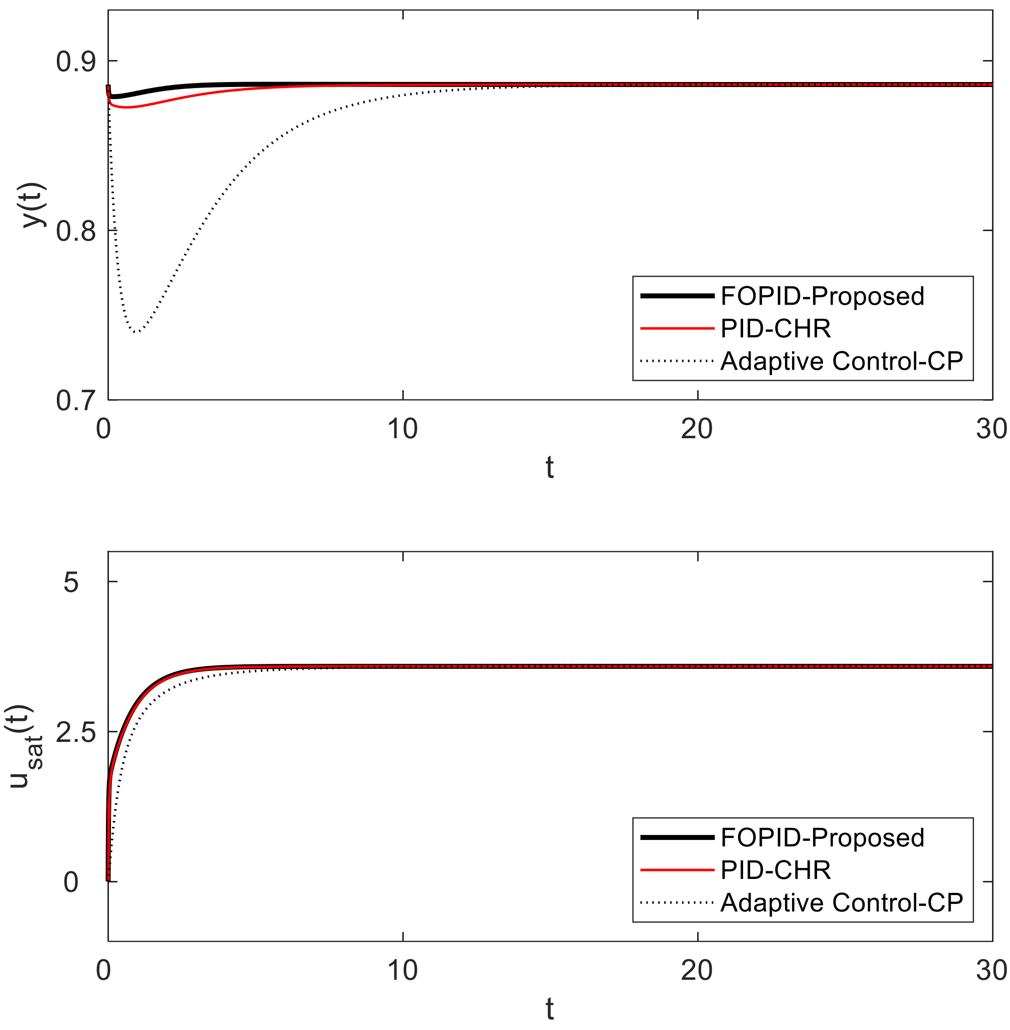

Figure 5.11 Disturbance rejection response

Table 5.12 Quantitative performance to step-type disturbance of d_1= 0.5 and d_2= -0.5.

Methods	Performance indices			
	t_{peak}	M_{peak}	t_{rcy}	IAE
FOID-Proposed	0.1935	0.0071	7.3426	0.0021
PID-CHR	0.6300	0.0134	9.0116	0.0441
Adaptive control-CP	0.9500	0.1460	11.9797	0.5887

5.6.2 Response to Scenario 2

The result of disturbance rejection response for step type change of d_1 from 0 to -0.5 and d_2 from 0 to 0.5 for the three methods is shown in the Figure 5.12. For the sake of convinces with scenario 1 discussion, the set point is kept constant at 0.886.

The graphical result for the three regulators has been performed and shown in Figure 5.7. Based on the simulation result, the proposed fuzzy gain scheduling FOPID controller has a recovery time and overshoot of 7.3081 and 0.71% respectively. The additional parameters are listed in Table 5.13. As can be seen from the graphical and tabular results, the proposed method has better performance parameter results when disturbance is considered. The comparison performance parameter results of the three control methods are shown in Table 5.12. Therefore, in this case the performance of the proposed method also has better performance on the disturbance rejection.

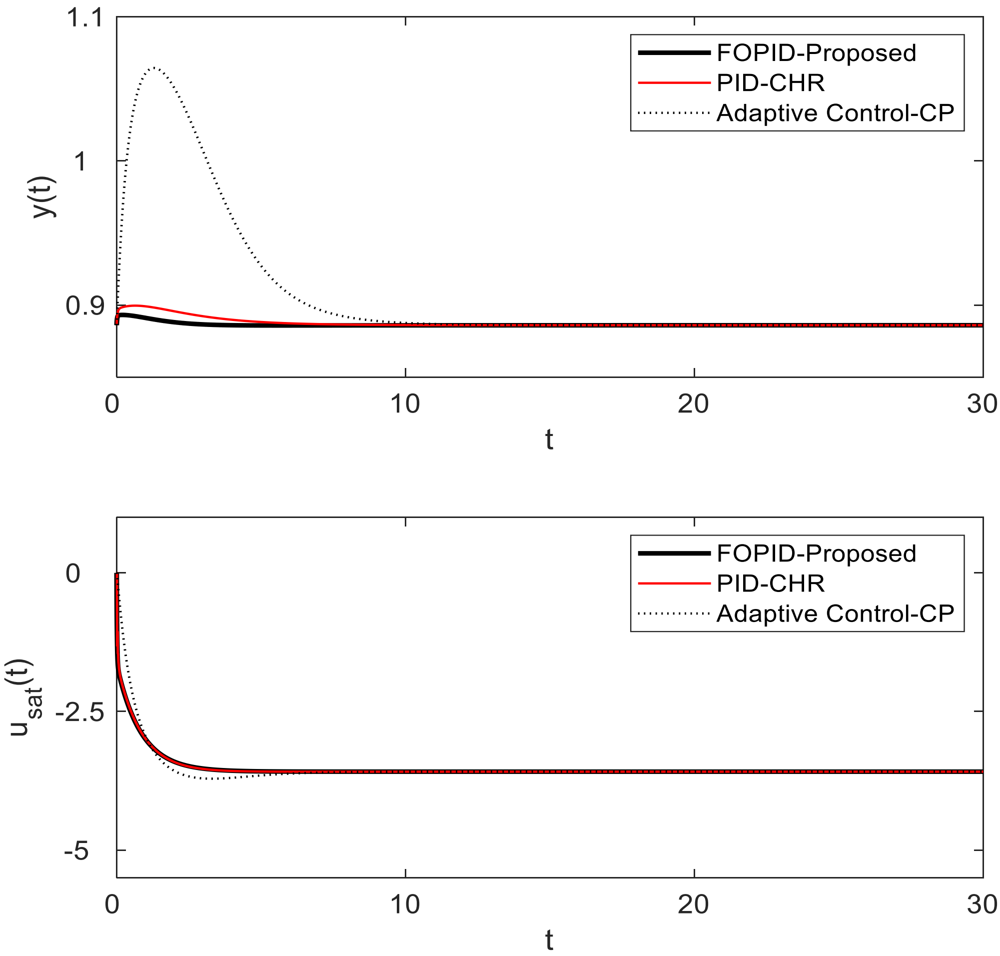

Figure 5.12 Disturbance rejection response

Table 5.13 Quantitative performance to step-type disturbance changes of d_1= -0.5 and d_2= 0.5.

Methods	Performance indices			
	t_{peak}	M_{peak}	t_{rcy}	IAE
FOPID-Proposed	0.1967	0.0071	7.3081	0.0021
PID-CHR	0.6400	0.0136	8.8868	0.0441
AC-CP	1.2900	0.1785	8.7094	0.6578

5.7. Summary

Form the simulation result and analysis, the proposed fuzzy gain scheduling FOPID controller has better performance in case of setpoint tracking and disturbance rejection capabilities than the other two existing methods implemented in this work. Also, as can be seen from this section, the proposed method has better performance as compared with the related works mentioned in Section 2.4.

CONCLUSION AND RECOMMENDATION

6.1 Conclusion

In this research work, the related works are reviewed and a CSTR process data are gathered from works of literature. Also, the mathematical modeling of both the proposed plant and controller has been done. Due to the complexity of system equations and parameters simplified dimensionless equations were formulated. The input/output relations of the temperature at a steady-state are highly nonlinear. It has three equilibrium points which are stable [0.1446, 0.8860], unstable [0.4472, 2.7517], and then stable [0.7646, 4.7050] points. Based on the proposed plant specifications the temperature can't be beyond the second point. As a result, only the first two operating regions (stable and unstable) were selected. Accordingly, two local FOPID controllers were designed for these two ranges.

This study presented the local controllers switching mechanism based on the operating ranges. A fuzzy gain scheduler was designed and a switching analysis has been done between the two local controllers (FOPID1 and FOPID2). The FOPID controller parameters were tuned by a genetic algorithm based on the IAEU. And also, their gains were selected based on the minimum value of the IAE. A Takagi Sugeno based fuzzy gain scheduler has been done.

Comparison between the proposed system and the two existing controllers which are Adaptive nonlinear and PID-CHR controllers were done based on setpoint tracking and disturbance rejection response. The comparison has been made based on the performance parameters criterion which is settling time, overshoot, rise time, and IAE. For the setpoint tracking response, the proposed controller results no overshoot and 1.0232 settling time for the first temperature range (0 to 0.886) and 4.8% overshoot and 2.45 settling time for the second operating range (0.886 to 2.7 517).

For disturbance rejection, when d_1 increase (0 to 0.5) and d_2 decrease from (0 to -0.5) with fixed setpoint (0.886), the proposed method has 7.1 % overshoot and recovery time of 7.3426. When d_1 decrease (0 to -0.5) and d_2 increase (0 to 0.5) with fixed setpoint (0.886) the proposed method had 0.71% overshoot ,7.3081 recovery time and 0.0021 IAE. The proposed fuzzy scheduled FOPID controller was outperformed other controllers in the case of setpoint tracking and disturbance rejection abilities.

In general, the contribution of this research work is designing of fuzzy gain scheduled FOPID controllers based on IAEU minimization in the respective operating ranges.

6.2 Recommendation

This work introduces the idea of the Fuzzy gain scheduling method of the FOPID controller to control the temperature of the CSTR process. The actual data for the proposed plant in this work were collected from different related works. Testing a proposed controller using real data is recommended. Also, for reducing the complexity in this study controlling of the concentration is not done. A cascade control system between the concentration and temperature of CSTR is recommended.

Research fund Acknowledgment

Research is fund by Adama Science and Technology University under the grant number ASTU/SM-R/163/20, Adama, Ethiopia.

REFERENCES

[1] W. L.Luyben, *Chemical reactor design and control*. Canada: John Wiley and Sons, 2007.

[2] R. E. Hayes and J. P. Mmbaga, *Introduction to chemical reactor analysis, second edition*. 2012.

[3] S. Moran and K.-D. Henkel, “Reactor Types and Their Industrial Applications,” *Ullmann’s Encycl. Ind. Chem.*, pp. 1–49, 2016, doi: 10.1002/14356007.b04_087.pub2.

[4] U. Mann, “Reactor Technology,” in *Kirk-Othmer Encyclopedia of Chemical Technology*, John Wiley and Sons, 2017, pp. 1–31.

[5] R. Ravi, *Reactor Design—General Principles*. Elsevier Ltd, 2017.

[6] A. B. de Haan, “4. Chemical reactors and their industrial applications,” in *Process Technology*, Berlin, München, Boston: De Gruyter, 2015, pp. 51–78.

[7] J. Butterfield, “Continuously Stirred Tank Reactors (CSTR),” [Online]. Available: https://www.sswnews.com/mobile/webarticles/2021/03/22/continuously-stirred-tank-reactors-cstr.html.

[8] L. Suo, J. Ren, Z. Zhao, and C. Zhai, “Study on the nonlinear dynamics of the continuous stirred tank reactors,” *Processes*, vol. 8, no. 11, pp. 1–18, 2020, doi: 10.3390/pr8111436.

[9] L. Xu and F. Ding, “Design of the PID controller for industrial processes based on the stability margin,” *Proc. 28th Chinese Control Decis. Conf. CCDC 2016*, pp. 3300–3304, 2016, doi: 10.1109/CCDC.2016.7531552.

[10] B. Platzer, “Chemical Reactor, Design and Control,” *Chemie Ing. Tech.*, vol. 82, no. 8, pp. 1266–1266, 2010, doi: 10.1002/cite.201090073.

[11] R. Ravi, R. Vinu, and S. N. Gummadi, *Coulson and Richardson’s Chemical Engineering, Fourth Edition Volume 3A Chemical and Biochemical Reactors and Reaction Engineering by R. Ravi, R. Vinu, S. N. Gummadi (z-lib.org)*, vol. 3A 4th Ed. 2017.

[12] A. Singh and V. Sharma, “Concentration control of CSTR through fractional order PID controller by using soft techniques,” *2013 4th Int. Conf. Comput. Commun. Netw. Technol. ICCCNT 2013*, 2013, doi: 10.1109/ICCCNT.2013.6726501.

[13] V. Vishnoi, S. Padhee, and G. Kaur, “Controller Performance Evaluation for Concentration Control of Isothermal Continuous Stirred Tank,” *Int. J. Sci. Res. Publ.*, vol. 2, no. 6, pp. 1–7, 2012.

[14] U. Mann, *Principles of Chemical Reactor and Anaysis and Design*, Second edi. Canda: John Wiley & Sons, Inc., Hoboken, New Jersey Published, 2009.

[15] the free encyclopedia Wikipedia, “Continuous stirred-tank reactor.” https://en.wikipedia.org/wiki/Continuous_stirred-tank_reactor.

[16] R. F. BIN ROSLAN, “Non-Isothermal Continuous Stirred Tank Reactor (Cstr) Using Fuzzy Logic Raihan Fikri Bin Roslan Chemical Engineering Universiti Teknologi Petronas,” no. September, 2015.

[17] P. R. Meghna, V. Saranya, and B. Jaganatha Pandian, “Design of Linear-Quadratic-Regulator for a CSTR process,” *IOP Conf. Ser. Mater. Sci. Eng.*, vol. 263, no. 5, 2017, doi: 10.1088/1757-899X/263/5/052013.

[18] R. Rao Alla, L. N, and R. K, “PID Control Design for Second Order Systems,” *Int. J. Eng. Manuf.*, vol. 9, no. 4, pp. 45–56, 2019, doi: 10.5815/ijem.2019.04.04.

[19] A. H. Halim and I. Ismail, “Tree physiology optimization on SISO and MIMO PID control tuning,” *Neural Comput. Appl.*, vol. 31, no. 11, pp. 7571–7581, 2019, doi: 10.1007/s00521-018-3588-9.

[20] D. S. Nagaraju and G. Ramesh, “Design and Implementation of Intelligent Controller for a Continuous Stirred Tank Reactor,” *Int. J. Res. Appl. Sci. Eng. Technol.*, vol. 2, no. Xi, pp. 474–482, 2014.

[21] M. Shahrokhi and A. Zomorrodi, “Comparison of PID Controller Tuning Methods,” *Dep. Chem. Pet. Eng. Sharif Univ. Technol.*, pp. 1–12, 2013.

[22] C. T. Chen and S. T. Peng, “Learning control of process systems with hard input constraints,” *J. Process Control*, vol. 9, no. 2, pp. 151–160, 1999, doi: 10.1016/S0959-1524(98)00038-9.

[23] V. Agarwal, A. Deo, N. Kumar, I. Volume, I. May, and P. No, “Temperature control of CSTR using PID Controller,” vol. 4, no. 5, pp. 11902–11905, 2015.

[24] I. Journal and O. F. Scientific, “Pid Controller Design For Cstr Plant Using Genetic Algorithm Based Pid Controller,” vol. 9, no. 03, pp. 652–655, 2020.

[25] M. Talwar, “Fuzzy Logic Based CSTR Control,” *Int. J. Adv. Eng. Res. Appl.*, vol. 1, no. 11, pp. 446–453, 2016.

[26] R. M. S. and D. P. Poongodi, “comparative analysis of various control statagies for a nonlinear CSTR system.pdf,” 2017.

[27] L. D. Swapnadeep Baruah, “Comparative study of PID based temperature control of CSTR using GA and PSO.pdf.” 2017.

[28] N. Khanduja, “Optimal design of FOPID Controller for the control of CSTR by using a novel hybrid metaheuristic algorithm,” *Sādhanā*, vol. 0123456789, 2021, doi: 10.1007/s12046-021-01632-1.

[29] I. C. J. Rajendra Murmu, “Design And Analysis of Intelligent Controller For Temperature Control In CSTR System,” *Int. J. Sci. Res. Educ.*, vol. 4, no. 7, pp. 5591–5597, 2016, doi: 10.18535/ijsre/v4i07.08.

[30] P. Kalita and J. K. Barman, “Performance Analysis of Non-linear Jacketed CSTR based on Different Control Strategies,” vol. 1, no. 2, pp. 1–7, 2017.

[31] N. Khanduja, “CSTR Control by Using Model Reference Adaptive Control and PSO,” *World Acad. Sci. Eng. Technol. Int. J. Mech. Aerospace, Ind. Mechatron. Manuf. Eng. Vol8, No12, 2014*, vol. 8, no. 12, pp. 2144–2149, 2014.

[32] A. Imam, “ANALYSIS OF LINEAR CONTROL FOR NONLINEAR SYSTEM: CONTINUOUS STIRRED TANK REACTOR (CSTR),” *J. Chem. Inf. Model.*, vol. 53, no. 9, pp. 1689–1699, 2013.

[33] N. Kumar and N. Khanduja, “Mathematical modelling and simulation of CSTR using MIT rule,” *India Int. Conf. Power Electron. IICPE*, 2012, doi: 10.1109/IICPE.2012.6450458.

[34] A. Sinha and R. K. Mishra, “Control of a nonlinear continuous stirred tank reactor via event triggered sliding modes,” *Chem. Eng. Sci.*, vol. 187, pp. 52–59, 2018, doi:

10.1016/j.ces.2018.04.057.

[35] W. H. Ray, *Advanced Process Control*. New York: McGraw-Hill, 1981.

[36] M. Galluzzo and B. Cosenza, “Control of a non-isothermal continuous stirred tank reactor by a feedback-feedforward structure using type-2 fuzzy logic controllers,” *Inf. Sci. (Ny).*, vol. 181, no. 17, pp. 3535–3550, 2011, doi: 10.1016/j.ins.2011.03.023.

[37] K. Aseem and M. P. Subeekrishna, “Comparitive Study of PID and Fractional Order PID Controllers for Industrial Applications,” vol. 7, no. 01, pp. 1–3, 2019.

[38] I. Podlubny, “Fractional Differential Equations; An Introduction to Fractional Derivatives, Fractional Differential Equations, to Methods of their Solution and some of their Application,” *book*, vol. 198, p. 283, 1999.

[39] M. A. K. El-Shafei, M. I. El-Hawwary, and H. M. Emara, “Implementation of fractional-order PID controller in an industrial distributed control system,” *2017 14th Int. Multi-Conference Syst. Signals Devices, SSD 2017*, vol. 2017-Janua, no. March 2017, pp. 713–718, 2017, doi: 10.1109/SSD.2017.8167004.

[40] N. Zhuo-Yun, Z. Yi-Min, W. Qing-Guo, L. Rui-Juan, and X. Lei-Jun, “Fractional-Order PID Controller Design for Time-Delay Systems Based on Modified Bode’s Ideal Transfer Function,” *IEEE Access*, vol. 8, pp. 103500–103510, 2020, doi: 10.1109/ACCESS.2020.2996265.

[41] M. V. A. and A. S. J. Ruchi V. Jainl, “Tuning of Fractional Order PID Controller Using Particle Swarm Optimization Technique for DC Motor Speed Control,” vol. 006, no. 2, pp. 6–9, 2016.

[42] B. Saidi, M. Amairi, S. Najar, and M. Aoun, “Bode shaping-based design methods of a fractional order PID controller for uncertain systems,” *Nonlinear Dyn.*, vol. 80, no. 4, pp. 1817–1838, 2015, doi: 10.1007/s11071-014-1698-1.

[43] F. Padula and A. Visioli, *Advances in robust fractional control*. 2015.

[44] A. Jayachitra and R. Vinodha, “Genetic Algorithm Based PID Controller Tuning Approach for Continuous Stirred Tank Reactor,” *Adv. Artif. Intell.*, vol. 2014, pp. 1–8, 2014, doi: 10.1155/2014/791230.

[45] A. Devanshu, “Genetic Algorithm Tuned PID Controller for Process Control,” *Int.*

Conf. Inven. Syst. Control., vol. 53, 2017.

[46] A. Soukkou, A. Khellaf, S. Leulmi, and K. Boudeghdegh, “Optimal control of a CSTR process,” *Brazilian J. Chem. Eng.*, vol. 25, no. 4, pp. 799–812, 2008, doi: 10.1590/S0104-66322008000400017.

[47] N. Bayati, A. Dadkhah, B. Vahidi, S. Hossein, and H. Sadeghi, “Fopid Design for Load - Frequency Control Using Genetic Algorithm,” *Sci . Int . (Lahore),* vol. 27, no. 4, pp. 3089–3094, 2015.

[48] C. Engineering, “Design of Fractional Order PID Controller Using Genetic Algorithm Optimization Technique for Nonlinear System,” pp. 1–11, 2020, doi: 10.1515/cppm-2019-0072.

[49] J. Poovarasan, R. Kayalvizhi, and R. K. Pongiannan, “Design of Fractional Order PID controller for a CSTR process,” vol. 3, no. 1, pp. 8–14, 2014.

[50] J.Jebakumar, K.Mishra, and B.MISHRA, “Controller Selection and Sensitivity Check on the Basic of Performance Index Calculation,” *Int. J. Electr. Electron. Data Commun.*, vol. 2, no. 1, pp. 91–93, 2014.

[51] S. Das, I. Pan, S. Das, and A. Gupta, “Engineering Applications of Artificial Intelligence A novel fractional order fuzzy PID controller and its optimal time domain tuning based on integral performance indices,” *Eng. Appl. Artif. Intell.*, vol. 25, no. 2, pp. 430–442, 2012, doi: 10.1016/j.engappai.2011.10.004.

[52] A. O. Shuaib and M. M. Ahmed, “Robust PID Control System Design Using ITAE Performance Index (DC Motor Model),” vol. 3, no. 8, pp. 15060–15067, 2014, doi: 10.15680/IJIRSET.2014.0308002.

[53] D. J. Leith and W. E. Leithead, “Survey of gain-scheduling analysis and design,” *Int. J. Control*, vol. 73, no. 11, pp. 1001–1025, 2000, doi: 10.1080/002071700411304.

[54] V. Bagyaveereswaran and P. Arulmozhivarman, “Gain scheduling of a robust setpoint tracking disturbance rejection and aggressiveness controller for a nonlinear process,” *Processes*, vol. 7, no. 7, 2019, doi: 10.3390/pr7070415.

[55] P. Aravind, M. Valluvan, and M. Saranya, “Simulation based Modeling and Implementation of Adaptive Control Technique for Non Linear Process Tank,” *Int. J. Comput. Appl.*, vol. 68, no. 16, pp. 1–6, 2013, doi: 10.5120/11660-7242.

[56] B. kr. Maurya and S. kr. Bajpai, “Fuzzy Logic Based Temperature Control of Continuous Stirred Tank Reactor,” *Int. J. Eng. Trends Technol.*, vol. 12, no. 2, pp. 109–112, 2014, doi: 10.14445/22315381/ijett-v12p219.

[57] A. Benzaouia, “Advanced Takagi–Sugeno Fuzzy Systems- Delay and Saturation (PDFDrive).pdf.” 2014.

[58] T. Yulianto, S. Komariyah, and N. Ulfaniyah, “Application of fuzzy inference system by Sugeno method on estimating of salt production,” *AIP Conf. Proc.*, vol. 1867, no. August 2017, 2017, doi: 10.1063/1.4994442.

Appendix

Appendix A: for mathematical modeling of CSTR Process

MATLAB code for the Equilibrium state and

```
%% Find the equilibrium states of the CSTR process
function graphES
clf
global Da gamma H beta
Da= 0.072; gamma= 20; H= 8; beta= 0.3;
% Plot the graph of x2 vs f(x2) at any u
u= 0;
x2= -5:0.01:5;
plot(x2,fun(x2,u),'k','linewidth',2)
xlabel('x_2'); ylabel('f(x_2)');
grid on
% Find the ES at u= 0
u= 0;
x20= [0 1];%[1.8 3.8];  %[-2 1.8]; %[3.8 7];
x2= fzero(@(x2) fun(x2,u), x20);
x1= (1+beta)*x2/H-beta*u/H;
[x1 x2]
function f= fun(x2,u)
global Da gamma H beta
x1= (1+beta)*x2/H-beta*u/H;
temp= exp(x2./(1+x2/gamma));
f= -x1+Da*(1-x1).*temp;
```

MATLAB coding for Phase diagram of CSTR process

```
%% phase diagram of the CSTR process
function SimEquPoint
```

```
t= 0; x0= [datas]; u= 0; h= 0.02; loop= 1000;
=0.7646; equ points= [xa1 xa2; xb1 xb2; xc1 xc2]
for k= 1:length(x0)
    x= x0(:,k);
    buf= x';
    for i= 1:loop
        x= RK4(@cstr,t,x,u,h);
        t= t+h;
        buf= [buf; x'];
    end
    hold on
    plot(buf(:,1),buf(:,2),'linewidth',1)
    axis([0 1 0 7])
end
plot(xa1,xa2,'o')
plot(xb1,xb2,'or')
plot(xc1,xc2,'o')
xlabel('x_1');ylabel('x_2');
```

MATLAB code for the open-loop response

```
function Openloop response
clf
t= 0; h= 0.01; loop= 2000;
x= [0.0672;0];
u0= SSInput(x)
buf= [t x'];
for i= 1:loop
    u= 0;
    % Calls the Saturation
    usat= Saturation(u,[-5 5])
```

```
    x= RK4(@CSTR,t,x,usat,h);
    t= t+h;
    buf= [buf; t x'];
end
plot(buf(:,1),buf(:,3),'k','linewidth',2)
axis([0 h*loop 0 1])
grid on
xlabel('t');ylabel('x_2(t)');
```

% Calls the CSTR process

MATLAB code for the steady-state response

```
% Draw the states of the CSTR in the steady-state
function Steady State CSTR
global Da gamma H beta
Da= 0.072; gamma= 20; H= 8; beta= 0.3;
buf= [];
for u= -5:0.005:5
    if u >=-0.515 && u<= 0.515
        x2= fzero(@(x) fun(x,u),[-2 1.8]);
        x1= (1+beta)/H*x2-beta/H*u;
        buf= [buf; u x1 x2];
        x2= fzero(@(x) fun(x,u),[1.8 3.8]);
        x1= (1+beta)/H*x2-beta/H*u;
        buf= [buf; u x1 x2];
        x2= fzero(@(x) fun(x,u),[3.8 7]);
        x1= (1+beta)/H*x2-beta/H*u;
        buf= [buf; u x1 x2];
    else
        x2= fzero(@(x) fun(x,u),[-2 8]);
        x1= (1+beta)/H*x2-beta/H*u;
```

```
        buf= [buf; u x1 x2];
    end
end
subplot 211
plot(buf(:,1),buf(:,2),'k.','linewidth',2)
hold on
xp= [0 0 0]; yp= [0.1440 0.4472 0.7646];
plot(xp,yp,'ro','linewidth',2)
xlabel('u(t)'); ylabel('x_1(t)');
grid on
hold off
subplot 212
plot(buf(:,1),buf(:,3),'k.','linewidth',2)
hold on
xp= [0 0 0]; yp= [0.8860 2.7517 4.7050];
plot(xp,yp,'ro','linewidth',2)
xlabel('u(t)'); ylabel('x_2(t)');
grid on
hold off
function f= fun(x2,u)
global Da gamma H beta
x1= (1+beta)/H*x2-beta/H*u;
temp= exp(x2./(1+x2/gamma));
f= -x1+Da*(1-x1).*temp;
```

Appendix B Appendix related to controller design

MATLAB code for FOPID1 and FOPID2 controller parameter tuning using GA

```
function Tune_FOPID_SP
clear all
```

```
rng default
options= optimoptions('ga','PlotFcn',@gaplotbestf);
options.PopulationSize= 30;
options.MaxGenerations= 30;  % Increase value if needed
nvar= 5; % Number of parameters
LB= [0 0 0 0 0]; % Lower bound of tuning parameters
UB= [30 30 10 2 2]; % Upper bound of tuning parameters
[x,fval]= ga(@EvalObj,nvar,[],[],[],[],LB,UB,[],options)
% Measures a performance index from the simulink model
function obj= EvalObj(x)
% Updates the values of Kp, Ki and Kd in Simulink model workspace
simulink_model= 'FOPID_Model1';
load_system(simulink_model);
gains= get_param(simulink_model,'modelworkspace');
% x10= 0.0672; x20= 0; yr= 0.886;
%  u0= -1.7910; % (1)
 x10= 0.1440; x20= 0.8860; yr= 2.7517;
 u0= 1.6605e-04;  % (2)
% calls gain assignments
gains.assignin('Kp', x(1));
gains.assignin('Ki', x(2));
gains.assignin('Kd', x(3));
gains.assignin('Lamda', x(4));
gains.assignin('mu', x(5));
gains.assignin('x10', x10);
gains.assignin('x20', x20);
% Simulates the simulink model to get the outputs
simOut= sim(simulink_model,'SaveOutput','on');
% Retrieves time t and error e
```

```
t= simOut.find('t');
e= simOut.find('e');
u= simOut.find('u');
```
% Calculate a performance index using the trapezoidal integration rule
```
w= 0.01; n= length(e);
ae= abs(e); au= w*abs(u-u0);
obj= 0;
for i= 2:n
    stepsize= t(i)-t(i-1);
    obj= obj+0.5*stepsize*(ae(i-1)+ae(i)+au(i-1)+au(i)); % IAEU
end
```
MATLAB code for gain scheduling method

```
%% Simulate the tuned FOPID control system for a step change
p1= [10.6322   12.9468    7.0947    0.7211  0.2899]; %fval = 1.0776, yr= 0 <->0.886
p2= [0.3851   10.9436    2.4501    0.0238 0.4019]; %fval = 2.5283, yr= 0.886 <-> 2.7517
%    x10= 0.0672; x20= 0; no= 1;% (1)
   x10= 0.0672; x20= 0; no= 2;% (2)
   u0= -1.7910; % (1), (2)
%    x10= 0.4472; x20= 2.7517; no= 3; % (3)
%  x10= 0.4472; x20= 2.7517; no= 4; % (4)
%   u0= 1.6605e-04;  % (3), (4)
simulink_model= 'FOPID_Model2';
load_system(simulink_model);
gains= get_param(simulink_model,'modelworkspace');
```
% Calls the CSTR

% calls FOPID1 gain assignments

% calls FOPID2 gain assignments

```
% Simulates the simulink model to get the outputs
simOut= sim(simulink_model,'SaveOutput','on');
```

```
% Retrieves t and y
buf= simOut.find('buf');
t= buf.Time;
% y1= buf.Data(:,1);
y2= buf.Data(:,2); % Temperature
u= buf.Data(:,3);
usat= buf.Data(:,4);
e= buf.Data(:,5);
% subplot 211
plot(t,y2,'linewidth',2)
 axis([0 15 0 3])
xlabel('t'), ylabel('y(t)')
% subplot 212
% plot(t,usat,'linewidth',2)
% xlabel('t'), ylabel('u(t)')
% Calculate a performance index using the trapezoidal integration rule
w= 0.01; n= length(e);
ae= abs(e)+w*abs(u-u0);
obj= 0;
for i= 2:n
    stepsize= t(i)-t(i-1);
    obj= obj+0.5*stepsize*(ae(i-1)+ae(i)); % IAEU
end
obj
% Save data
% buf= [t y1 y2 usat];
```

Appendix C: MATLAB SIMULINK model

Appendix C.2 PID-CHR controller based CSTR process

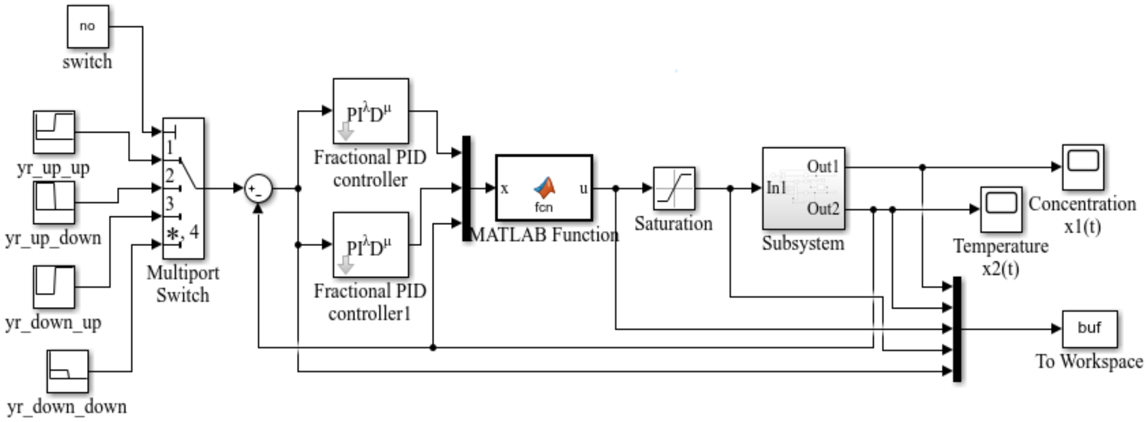

Figure C.1 MATAB Simulink of proposed control system.

Appendix C.2 PID-CHR controller based CSTR process

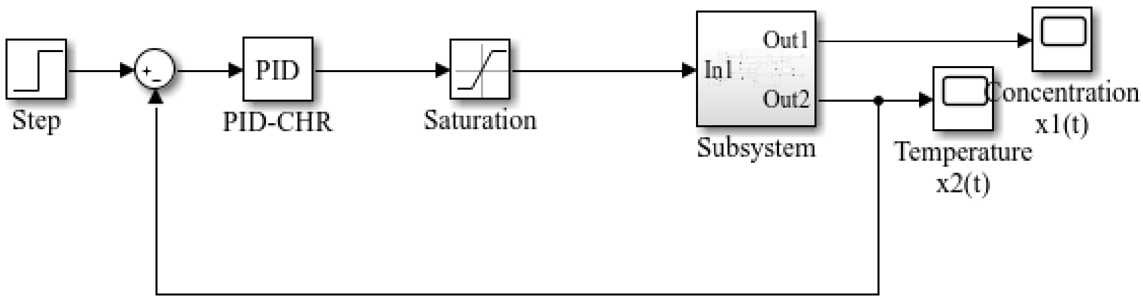

Figure C.2 MATAB Simulink of PID-CHR control system.

Appendix C.3 Nonlinear adaptive control based CSTR process

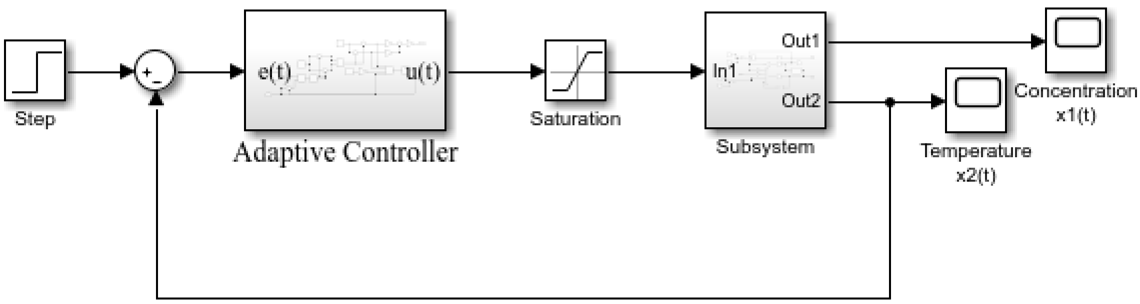

Figure C.3 MATAB Simulink of adaptive nonlinear control system.